

Laser Vision: Lidar as a Transformative Tool to Advance Critical Zone Science

Adrian A. Harpold*, University of Nevada, Reno, aharpold@email.arizona.edu

Jill A. Marshall, University of Oregon, jillm@uoregon.edu

Steve W. Lyon, Stockholm University, steve.lyon@natgeo.su.se

Theodore B. Barnhart, University of Colorado, theodore.barnhart@colorado.edu

Beth Fisher, University of Minnesota, wene0018@umn.edu

Mitchell Donovan, University of Maryland – Baltimore County, mdonovan@umbc.edu

Kristen M. Brubaker, Hobart and William Smith Colleges, brubaker@hws.edu

Christopher J. Crosby, UNAVCO, Crosby@unavco.org

Nancy F. Glenn, Boise State University, nancyglenn@boisestate.edu

Craig L. Glennie, University of Houston, clglenni@central.uh.edu

Peter B. Kirchner, University of California, Los Angeles, peter.b.kirchner@jpl.nasa.gov

Norris Lam, Stockholm University, norris.lam@natgeo.su.se

Kenneth D. Mankoff, Woods Hole Oceanographic Institute, kmankoff@whoi.edu

James L. McCreight, National Center for Atmospheric Research, mccreigh@gmail.com

Noah P. Molotch, University of Colorado, Boulder, noah.molotch@colorado.edu

Keith N. Musselman, University of Saskatchewan, keith.musselman@usask.ca

Jon Pelletier, University of Arizona, jon@geo.arizona.edu

Tess Russo, Pennsylvania State University, russo@psu.edu

Harish Sangireddy, University of Texas, Austin, hsangireddy@utexas.edu

Ylva Sjöberg, Stockholm University, ylva.sjoberg@natgeo.su.se

Tyson Swetnam, University of Arizona, tswetnam@email.arizona.edu

Nicole West, Pennsylvania State University, nxw157@psu.edu

*Corresponding author: Adrian A. Harpold, aharpold@cabnr.unr.edu

Laser Vision: Lidar as a Transformative Tool to Advance Critical Zone Science

1
2 Observation and quantification of the Earth surface is undergoing a revolutionary change due to
3 the increased spatial resolution and extent afforded by light detection and ranging (lidar)
4 technology. As a consequence, lidar-derived information has led to fundamental discoveries
5 within the individual disciplines of geomorphology, hydrology, and ecology. These disciplines
6 form the cornerstones of Critical Zone (CZ) science, where researchers study how interactions
7 among the geosphere, hydrosphere, and biosphere shape and maintain the 'zone of life',
8 extending from top of unweathered bedrock to the top of the vegetation canopy. Fundamental to
9 CZ science, is the development of transdisciplinary theories and tools that transcend individual
10 disciplines and inform other's work, capture new levels of complexity, and create new
11 intellectual outcomes and spaces. Researchers are just beginning to utilize lidar datasets to
12 answer synergistic, transdisciplinary questions in CZ science, such as how CZ processes co-
13 evolve over long-time scales and interact over shorter time scales to create thresholds shifts in
14 states and fluxes of water, energy, and carbon. The objective of this review is to elucidate the
15 transformative potential of lidar for CZ science to simultaneously allow for quantification of
16 topographic, vegetative, and hydrological processes. A review of 147 peer-reviewed studies
17 utilizing lidar highlights a lag in utilizing lidar for CZ studies as 38% of the studies were focused
18 in geomorphology, 18% in hydrology, 32% in ecology, and the remaining 12% had an
19 interdisciplinary focus. A handful of exemplar transdisciplinary studies demonstrate that well-
20 integrated lidar observations can lead to fundamental advances in CZ science, such as
21 identification of feedbacks between hydrological and ecological processes over hillslope scales
22 and the synergistic co-evolution of landscape-scale CZ structure due to interactions amongst
23 carbon, energy, and water cycles. We propose that using lidar to its full potential will require

24 numerous advances across CZ applications, including new and more powerful open-source
25 processing tools, exploiting new lidar acquisition technologies, and improved integration with
26 physically-based models and complementary *in situ* and remote-sensing observations. We
27 provide a five-year vision that advocates for the expanded use of lidar datasets and highlights
28 subsequent potential to advance the state of CZ science.

29

30 **1. INTRODUCTION**

31 Complex interactions among the geosphere, ecosphere, and hydrosphere give rise to present-day
32 landforms, vegetation, and corresponding water and energy fluxes. Critical Zone (CZ) science
33 studies these interactions in the zone extending from top of unweathered bedrock to the top of
34 the vegetation canopy. Understanding CZ function is fundamental to characterizing regolith
35 formation, carbon-energy-water cycles, meteorological controls on ecology, linked surface and
36 subsurface processes, and numerous other Earth surface processes (NRC, 2012). Improved
37 understanding of CZ functions is thus important for quantifying ecosystem services and
38 predicting their sensitivity to environmental change. However, CZ processes are difficult to
39 observe because they occur over time scales of seconds to eons and spatial scales of centimeters
40 to kilometers, and thus require diverse measurement approaches (Chorover et al., 2011). Light
41 detection and ranging (lidar) technologies can be helpful in this regard because they generate
42 repeatable, precise three-dimensional information of the Earth's surface characteristics.

43

44 Lidar allows for simultaneous measurements of aboveground vegetation structure and human
45 infrastructure, as well as the topography of the earth surface, including soils, exposed bedrock,
46 stream channels, and snow/ice. Depending on the data collection system and platform,

47 observations can be made at the landscape scale ($>1000 \text{ km}^2$) and at spatial resolutions capable
48 of capturing fine-scale processes ($<10 \text{ cm}$). These unique measurement capabilities offered by
49 lidar have the potential to lead to transdisciplinary research questions, which transcend a single
50 discipline, capture greater complexity, and create new intellectual advances that are synergistic
51 (across disciplines) in nature. Fundamental CZ science questions often require transdisciplinary
52 approaches that surpass what is possible in multidisciplinary (i.e. collaborations across
53 disciplines that pose their own questions) or interdisciplinary (i.e. collaborations where
54 information is transferred amongst disciplines) research settings. Because lidar can characterize
55 geomorphic, ecologic, and hydrologic processes simultaneously across a range of scales, it is
56 uniquely suited to address questions posed by CZ research.

57

58 Lidar acquisition capabilities are increasing exponentially (Stennett, 2004; Glennie et al., 2013)
59 and new ground-based (terrestrial laser scanning, TLS), mobile platforms (airborne laser
60 scanning, ALS or other mobile platforms like a truck or boat), and space-based platforms
61 (spaceborne laser scanning, SLS) are leading to increased availability of lidar datasets with CZ-
62 relevant information content. Different lidar platforms each have their own advantages and
63 limitations, but operate based on a similar principle by emitting and measuring the time of travel
64 of an energy pulse (laser light) and thus, measuring and mapping distance to a target. Collection
65 via TLS methods typically involves lidar scanners that are mounted on tripods or other fixed
66 locations. Fixed targets are used to georeference the lidar datasets, with a high resolution GPS, to
67 composite multiple TLS scans into a single point cloud. TLS scanners are becoming more
68 affordable and available to individual researchers and groups. lidar collections via mobile
69 platforms are typically performed by mounting the lidar unit on an aircraft, helicopter, or vehicle

70 that is moved over the study area of interest. The aircraft must be equipped with a GPS unit and
71 Internal Measurement Unit (IMU) to track the orientation and location of the scanner. Similar to
72 TLS collection, ALS methods require ground targets with known GPS locations for
73 georeferencing. Lidar collection via SLS are much less common, but have been successfully
74 deployed on orbiting spacecraft, and will become more prevalent in 2017 with the planned
75 launch of ICESat-2 (Abdalati et al., 2010). In addition to the laser system, the spacecraft must
76 have a GPS unit and altitude determination system in order to georeference the data. Each of
77 these lidar platforms offer specifications that can be selected and adjusted for a given science
78 application. Throughout this review we present studies using the suite of lidar methods and
79 highlight the advantages of each method for differing scientific purposes.

80

81 The objective of this paper is to present a five-year vision for applying lidar to advance
82 transdisciplinary CZ research. To accomplish this we first present the state of the science on
83 applying lidar to disciplinary-specific research in geomorphology, hydrology, and ecology in
84 Sections 1.1, 1.2, and 1.3, respectively. This is followed in Section 2.1 by an exploration of
85 transdisciplinary studies that utilized complementary lidar-derived datasets to propel CZ science
86 beyond what is possible within disciplinary endeavors. We summarize these exemplar
87 transdisciplinary studies with the intent to guide future research. In Section 2.2 we describe how
88 lidar-derived information is uniquely suited to advance three CZ research topics beyond the
89 current state of the science: 1) quantifying change detection, 2) parameterization and verification
90 of physical models, and 3) improved understanding of CZ processes across multiple scales.
91 These topics are limited by a set of common impediments that we outline in Section 2.3. Finally,
92 in Section 2.4, we present a vision to advance CZ science with lidar using examples of

93 transdisciplinary research questions and provide a set of recommendations for the CZ community
94 to increase usage and advocate for greater lidar resources over the next five years.

95

96 **1.1 Advances in Geomorphology Using Lidar**

97 High-resolution topographic datasets derived from lidar have greatly contributed to quantifying
98 geomorphic change, identifying geomorphic features, and understanding ecohydrologically-
99 mediated processes at varying scales and extents. These advances have allowed testing of
100 geomorphic models, pattern and process recognition, and the identification of unanticipated
101 landforms and patterns (e.g. waveforms) that were not possible using previous survey
102 techniques. Generally, lidar information complements rather than replaces field observations,
103 with lidar observations leading to new hypothesis and process cognition (Roering et al., 2013).
104 Broadly, lidar technology has been useful in studying geomorphic response to extreme events
105 such as fire and storms (e.g., Pelletier and Orem, 2014; Sankey et al., 2013; Perignon et al.,
106 2013; Staley et al., 2014), human activities (e.g. James et al., 2009), and past climatic and
107 tectonic forcings (e.g., Roering, 2008; Belmont, 2011; West et al., 2014). Meter and sub-meter
108 scale time-varying processes, often derived from TLS, have been quantified in the response of
109 point bar and bank morphodynamics (Lotsari et al., 2014) and in the formation of
110 microtopography due to feedbacks with biota (e.g., Roering et al., 2010; Pelletier et al., 2012;
111 Harman et al., 2014). Examples of larger scale change detection applications, typically ALS-
112 derived, include measuring changes in stream channel pathways resulting from Holocene climate
113 change and anthropogenic activities (e.g., Day et al., 2013; Kessler, 2012; James 2012; Belmont
114 et al., 2011), rates of change in migrating sand dunes (Pelletier, 2013), the influence of lithology
115 and climate on hillslope form (e.g., Marshall and Roering, 2014; Hurst et al., 2013; Perron et al.,

116 2008; West et al., 2014), and channel head formation (e.g., Pelletier et al., 2013; Pelletier and
117 Perron, 2012; Perron and Hamon, 2012). Automated tools to identify geomorphic features (i.e.,
118 floodplains, terraces, landslides) and transitional zones (i.e., hillslope-to-valley, floodplain-to-
119 channel) have been used in conjunction with high-resolution elevation datasets from lidar,
120 including Geonet 2.0 (Passalacqua et al., 2010), ALMTools (Booth et al., 2009), and TerrEX
121 (Stout and Belmont, 2014).

122

123 **1.2 Advances in Hydrology Using Lidar**

124 Research utilizing lidar has advanced fundamental process understanding in snow hydrology
125 (Deems et al., 2013), surface water hydraulics (Lane et al., 2004; Nathanson et al., 2012; Lyon et
126 al., 2015), and land-surface-atmosphere interactions (Mitchell et al., 2011). Lidar-derived snow
127 depths (derived by differencing snow-on and snow-off elevations) over large ($>1 \text{ km}^2$) spatial
128 extents from both ALS and TLS (Deems et al., 2013), have yielded unprecedented contiguous
129 maps of spatial snow distributions (e.g. Fassnacht and Deems, 2006; McCreight et al., 2014) and
130 provided new insights into underlying processes determining spatial patterns in snow cover
131 (Trujillo et al., 2009; Kirchner et al., 2014), accumulation and ablation rates (Grunewald et al.,
132 2010; Varhola and Coops, 2013), snow water resources for planning (Hopkinson et al., 2012),
133 and estimating the effects of forest cover and forest disturbance on snow processes (Harpold et
134 al., 2014a). Change detection techniques have been effective for determining glacier mass
135 balances (Hopkinson and Demuth, 2006), ice surface properties (Williams et al., 2013), and
136 calving front movements (e.g., Arnold et al., 2006; Hopkinson et al., 2006). Prior to lidar, many
137 of these cryospheric processes had to be investigated using single point observations or through
138 statistical rather than deterministic analyses; the additional information derived from lidar has

139 yielded important insights that advanced scientific understanding. High- resolution topographic
140 information from lidar has proved important for stream channel delineation (Kinzel et al, 2013),
141 rating curve estimation (Nathanson et al., 2012; Lyon et al., 2015), floodplain mapping and
142 inundation (Marks and Bates, 2000; Kinzel et al., 2007), and topographic water accumulation
143 indices (Sørensen and Seibert, 2007; Jensco et al., 2009). Lidar measurements of micro-
144 topography measured using lidar shows potential for improving soil property and moisture
145 information (e.g., Tenenbaum et al, 2006), surface and floodplain roughness (Mason et al., 2003,
146 Forzieri et al., 2010; Brasington et al., 2012; Brubaker et al., 2013), hydraulic dynamics and
147 sediment transport (Roering et al., 2012; McKean et al., 2014), surface ponding and storage
148 volume calculations (Li et al., 2011; French, 2003), and wetland delineation (e.g. Lane and
149 D’Amico, 2010). Certain hydrological modeling fields are well-poised to utilize high-resolution
150 topography, such as movement of water in urban environments (Fewtrell et al., 2008), in-channel
151 flow modeling (Mandlburger et al., 2009; Legleiter et al., 2011), and hyporheic exchange and
152 ecohydraulics in small streams (e.g. Jensco et al., 2009). Finally, high-resolution, three-
153 dimensional lidar measurements of canopy and vegetation structure (Vierling et al., 2008) have
154 direct implications for modeling the surface energy balance (Musselman et al., 2013) and
155 evapotranspiration processes (Mitchell et al., 2011) at scales critical to increasing fidelity in
156 physically-based models (Broxton et al., 2014).

157

158 **1.3 Advances in Ecology Using Lidar**

159 Lidar-based remote sensing of vegetation communities has transformed the way ecologists
160 measure vegetation across multiple spatial scales (e.g. Lefsky et al. 2002; Maltamo et al. 2014;
161 Streutker and Glenn 2006). Substantial work has been undertaken using lidar to map vegetation

162 structure and biomass distributions (see reviews by Seidel et al. 2011 and Wulder et al. 2012).
163 These include the estimation of Leaf Area Index (LAI) (Riaño et al. 2004, Richardson et al.
164 2009; Hopkinson et al., 2013), vegetation roughness (Strecker and Glenn, 2006; Antonarakis et
165 al., 2010), alpine tree lines (Coops et al., 2013), and total carbon storage and sequestration rates
166 in forest, grassland, savannahs and/or shrubland communities (Asner et al. 2012a, Baccini et al.
167 2012, Mascaro et al. 2011, Simard et al. 2011; Antonarakis et al., 2014). ALS has been used to
168 characterize wildlife habitat in tree and shrub canopies (Hyde et al. 2005, Bork and Su, 2007;
169 Vierling et al. 2008, Martinuzzi et al. 2009; Zellweger et al., 2014) and in aquatic systems
170 (McKean et al. 2008, Wedding et al. 2008, McKean et al., 2009). ALS has been a critical tool in
171 modeling catchment scale water-availability for vegetation at fine (Harmon et al. 2014) and
172 broad spatial scales (Chorover et al. 2011). Radiation transmission and ray-tracing models
173 utilizing lidar provide ecologists with better tools to quantify in-canopy and below-canopy light
174 environments (Lee et al., 2009; Bittner et al. 2014; Musselman et al. 2013; Bode et al., 2014;
175 Moeser et al., 2014). Additionally, ecologists are beginning to quantify the impact of vegetation
176 on micro-topography (Sankey et al. 2010; Pelletier et al., 2012; Harmon et al., 2014), as well as
177 larger landform processes (Pelletier et al. 2013). Broad-scale lidar data allows for quantification
178 of patches and mosaics amongst plant functional types across landscapes (Antonarakis et al.,
179 2010, Dickinson et al., 2014) and global forest biomass estimates (Simard et al., 2011).
180 Ecologists have fused data from hyperspectral imaging and lidar to enable species classification
181 for close to a decade (e.g. Mundt et al., 2006). However, new opportunities exist to link species-
182 level detail and plant functional response through emerging technologies, including co-
183 deployment of hyperspectral and lidar sensors (Asner et al. 2012b), and hyperspectral
184 (supercontinuum) laser technology (Kaasalainen et al. 2007, Hakala et al. 2012). By linking lidar

185 with additional observations, researchers have begun to quantify species-level detail and plant
186 health estimation (Cho et al. 2012, Féret and Asner 2012; Olsoy et al., 2014) and model forest
187 carbon fluxes (Antonarakis et al., 2014).

188

189 **2. Current Toolkits and Open Questions Using Lidar in CZ Science**

190 Research based on lidar-derived information accounts for substantial advances within the
191 cornerstone CZ disciplines. However, many open questions in CZ science require linked,
192 transdisciplinary investigations across multiple disciplines that create new intellectual spaces for
193 scientific advancements. For example: How do CZ processes co-evolve over long-time scales
194 and interact over shorter time scales to develop thresholds and shifts in states and fluxes of
195 water, energy, and carbon? What will be the response of the CZ structure to disturbance and land
196 use change? These CZ science questions must elucidate feedbacks and interactions among the
197 geosphere, ecosphere, and hydrosphere that cannot be accomplished within individual disciplines
198 (multidisciplinary) or sharing information across disciplines (interdisciplinary), but instead
199 require synergistic transdisciplinary science that spans multiple spatial and temporal scales.

200

201 A key advantage of lidar for understanding CZ feedbacks is the coupling of previously
202 unprecedented coverage over both broad temporal and spatial scales (Figure 1). The utility of
203 lidar for geo- eco- and hydro-sphere investigations is dependent on the platform (e.g. TLS, ALS,
204 or SLS) with cross-platform observations capable of resolutions from 10^{-3} m to continental scales
205 (Figure 1). In terms of temporal extent, TLS, ALS and SLS are capable of employing weekly to
206 sub-hourly repeat scan rates (Figure 1). Technologies allowing for faster scan rates will typically
207 limit the spatial extent (Figure 1). Advances in technology described in Section 2.3 will increase

208 the spatial and temporal resolutions for all lidar platforms in the next five years (Figure 1). The
209 intersecting process scales shown in Figure 1 demonstrate the viability of extracting
210 transdisciplinary information from lidar given thoughtful experimental design and data
211 collection.

212

213 **2.1 Lidar as Transdisciplinary CZ Tool**

214 To investigate the state of the science of lidar in CZ research we conducted a literature review of
215 147 peer-review papers that employed lidar datasets to improve process-based understanding in
216 the CZ domain. Our review found that most lidar studies to date have had a single disciplinary
217 objective and that the CZ community are less likely to utilize the overlapping information in
218 space and time generated by lidar available for transdisciplinary CZ advancement (Figure 1).
219 This is not surprising given the rampant progress made in filling important knowledge gaps in
220 the individual cornerstone CZ disciplines using lidar datasets (Sections 1.1 to 1.3). We organized
221 the literature reviewed for this paper into a scoring system of geomorphic, hydrologic, and
222 ecologic process knowledge advanced through individual lidar-based studies. For each paper we
223 assigned 10 points among the three disciplines to capture potential transdisciplinary lidar use.
224 For example, a study leading purely to hydrologic process advances would rank as 10 in the
225 hydrology category and zero in the ecology and geomorphology categories. A study balancing
226 the process-based inferences among the three disciplines, with a more prominent ecological
227 focus, would have been assigned scores of 3, 3, and 4 for geomorphology, hydrology, and
228 ecology, respectively. Of course, this is a subjective scaling based on author opinions. To limit
229 potential impacts of subjectivity, three different authors of the current paper assigned

230 independent scores to each study and we used the average score to place each paper in the
231 relative ranking triangle (Figure 2).

232

233 The motivation for developing the conceptualization in Figure 2 is to facilitate identification of
234 studies employing transdisciplinary synergies (e.g., lie within the internal triangle) that rely on
235 the multi-faceted nature of lidar datasets. The review showed 38% of 147 studies were focused
236 (score of 6 or higher) in geomorphology, 18% in hydrology, 32% in ecology, and the remainder
237 had a more interdisciplinary focus. The few studies in the center of the triangle (i.e., studies
238 receiving a minimum of 20% in each discipline) could be considered as potential exemplars of
239 CZ science using lidar as they balance well among each cornerstone discipline. Several studies
240 were transdisciplinary in nature, but focused on lidar-derived topography and did not maximize
241 information content on hydrological and ecological processes from lidar: Pelletier et al. (2012),
242 Persson et al. (2012), Brubaker et al. (2013), Pelletier (2013), Coops et al. (2013), Rengers et al.
243 (2014), and Pelletier and Orem (2014). We instead draw focus to transdisciplinary studies that
244 demonstrate the potential for complimentary information to be extracted from lidar and
245 integrated into field campaigns to allow multi-scale observations of interacting geomorphologic,
246 hydrologic, and ecologic processes.

247

248 We highlight three studies that can serve as possible roadmaps to guide future transdisciplinary
249 investigations using lidar datasets (Figure 2): Harman et al., 2014, Pelletier et al., 2013, and
250 Perignon et al., 2013. These studies used complimentary information from lidar to develop
251 fundamental transdisciplinary advances in the theories and understanding of CZ processes and
252 structure. For example, Harman et al. (2014) applied TLS to investigate coevolution of lidar-

253 derived microtopography and vegetation (biovolume) at two 100-m long semi-arid hillslopes.
254 Integrating lidar and limited field measurements, Harman et al. (2014) found that both alluvial
255 and colluvial processes were important in shaping vegetation and soil dynamics on hillslopes.
256 The insights found by Harman et al. (2014) relied on the high resolution and precision of lidar
257 information and would not have been possible using coarser traditional survey techniques for
258 topography and vegetation structure. Pelletier et al. (2013) investigated landscape-scale (>10
259 km²) variability in above-ground biomass, hydrologic routing, and topography derived from lidar
260 at two mountain ranges in southern Arizona and applied a landscape evolution model to
261 demonstrate the need to include ecological processes (e.g. vegetation density) to correctly model
262 topography. Lidar-derived vegetation structure provided new information not attainable from
263 other methods that allowed for Pelletier et al. (2013) to test a novel model of CZ development
264 based on eco-pedo-geomorphic feedbacks. Perignon et al. (2013) investigated topographic
265 change following a major flood along a 12 km stretch of the Rio Puerco in New Mexico. They
266 found that sedimentation patterns reflected complex interactions of vegetation, flow, and
267 sediment at the scale of individual plants. This example demonstrates the value of lidar for
268 testing ecohydrological resilience to extreme events to develop new understanding of the fine-
269 scale ecological feedbacks (i.e. individual plants) on reach scale geomorphic response.

270

271 These exemplar studies demonstrate the utility of lidar for transdisciplinary process
272 investigations at scales ranging from hillslopes (e.g. Harman et al., 2014), to stream reaches (e.g.
273 Perignon et al., 2013), to mountain ranges (e.g. Pelletier et al., 2013). We believe that these
274 exemplar transdisciplinary studies should serve as motivation for increased use of lidar and
275 integrated, multi-scale field observations for advancing CZ science. To this end, in Section 2.4

276 we provide additional examples to illustrate the overlapping processes observable with lidar that
277 are motivated by CZ science questions.

278

279 **2.2 Applying Lidar in CZ Science**

280 Through our literature review and subsequent conceptualizations (e.g., Figure 1) we have
281 identified three clear areas where lidar observations have the potential to advance the state of CZ
282 science in the next five years: 1) quantifying change detection, 2) parameterization and
283 verification of physical models, and 3) improved understanding of CZ processes across multiple
284 scales. Applying these tools is not mutually exclusive and each area has different levels of
285 previous research and development. For example, change detection utilizing lidar has received
286 notable use in the CZ science community, particularly by geomorphologists analyzing
287 topographic change over time. The use of lidar to quantify scaling relationships and thresholds
288 remains relatively unexplored, despite robust scaling theories and analysis tools from other fields
289 that are portable to lidar datasets. Similarly, integration of lidar datasets for either
290 parameterization or verification has had limited development within CZ-relevant models.

291

292 **2.2.1 Change Detection**

293 Lidar-based change-detection analyses (CDA), i.e. mapping landscape adjustments through time
294 in multi-temporal ALS and TLS datasets, have provided comprehensive measurements of snow
295 depth (e.g. Harpold et al., 2014b; Tinkham et al., 2014) and ablation (Egli et al., 2012), co-
296 seismic displacements after earthquakes (e.g. Oskin et al., 2012; Nissen et al., 2014), changes in
297 aeolian dune form and migration rates (e.g. Pelletier, 2013), fluvial erosion (e.g. Anderson and
298 Pitlick, 2014; Pelletier and Orem, 2014), earthflow displacements (e.g. DeLong et al., 2012),

309 knickpoint migration in gully/channel systems (e.g. Rengers and Tucker, 2014), cliff retreat
300 along coasts (Young et al., 2010), permafrost degradation (Levy et al., 2013; Barnhart and
301 Crosby, 2013), forest growth (Yu et al., 2004; Næsset and Gobakken, 2005), and changes in
302 biomass (e.g. Meyer et al. 2013; Olsoy et al., 2014). Traditionally, lidar point clouds have been
303 rasterized prior to differencing using open-source processing toolkits (e.g. GCD; e.g. Wheaton et
304 al., 2010). However, new methods such as Iterative Closest Point (Nissen et al., 2012), particle
305 image velocimetry (Aryal et al., 2012), and Multiscale Model to Model Cloud Comparison
306 (Lague et al., 2013) enable direct differencing of point clouds. Continued methodological
307 advances, coupled with increasingly available repeat datasets will progress the capabilities and
308 quality of CDA. Structure from Motion (SfM) estimates three-dimensional structures from two-
309 dimensional images providing an easily portable and low-cost method for making high-
310 frequency change detection measurements (Westoby et al., 2012; Fonstad et al., 2013). There is
311 also potential to apply time-series multi/hyperspectral lidar datasets to quantify changes in forest
312 health over time. Similarly, integration of bathymetric lidar with ALS opens the potential to
313 monitor dynamic changes in river flow and sediment transport (Flener et al., 2013). Although
314 researchers often implement CDA using historic datasets (Rhoades et al., 2009), challenges arise
315 from sparse metadata and reduced accuracy, thereby limiting dataset utility (e.g. Glennie et al.
316 2014). Future CDA may be improved by further establishing, through repositories such as
317 OpenTopography and UNAVCO, best practices for dataset sharing and archiving.

318

319 **2.2.2 Scaling CZ Processes**

320 While researchers have harnessed existing scaling theories and tools utilizing lidar datasets, there
321 is room for expansion using the range of scales afforded by lidar technologies (Figure 1). Two

322 complementary techniques, characterizing fractal patterns (e.g. Deems et al. 2006; Glenn et al.,
323 2006; Perron et al., 2008) and process changes expressed as fractal breaks (e.g. Drake and
324 Weishampel, 2000), benefit from the extensive breadth of spatial scales offered by lidar data.
325 Self-similar patterns across scales indicate consistent processes and thus provide a framework for
326 sampling, modeling, and re-scaling processes. Variograms and semi-variograms are commonly
327 employed to plot lidar-derived attributes of interest such as snow distribution (e.g. Deems et al.
328 2008; Harpold et al., 2014a) or forest spatial patterns (e.g. Boutet et al. 2003) against scale.
329 Fractal and fractal deviations, as well as the length-scales of landscape structure (Perron et. al.
330 2008), convey important CZ information, e.g., the effect of tree-root spacing through time on soil
331 production (Roering et al., 2010), patterns in tree gap-formation (Plotnick et al. 1996; Frazer et
332 al., 2005), and underlying abiotic and biotic controls on forest fractal dimensions (Drake and
333 Weishampel, 2000). Within the CZ framework, lidar allows consideration of topographic
334 variation and biomass distribution (Chorover et al. 2011), and spatial thresholds for interactions
335 among vegetation, hydrology, lithology, and surface processes ranging from the grain to
336 landscape scale (e.g., Musselman et al. 2013, Pelletier et al. 2013; Harman et al., 2014). Zhao et
337 al. (2009) developed a scale-invariant model of forest biomass, which illustrated the utility of
338 scale-independent methods. However, we caution that one scientist's signal may be another's
339 noise (Tarolli, 2014). Signal recognition may involve smoothing at one scale to quantify a
340 relevant landscape metric, such as hillslope curvature (and derived erosion rates) (Hurst et al.
341 2013), which in turn limits valuable information at another scale, such as hydrologically-driven
342 surface roughness or the spacing of tree-driven bedrock disruption (Roering et al. 2010, Hurst et
343 al 2012). Overall, lidar datasets retain the promise of up- or down- scaling feedbacks among
344 multiple processes that are just beginning to be fully utilized.

345
346
347
348
349
350
351
352
353
354
355
356
357
358
359
360
361
362
363
364
365
366
367

2.2.3 Model Parameterization and Verification

The wealth of recently collected lidar data has potential to inform the choice of physically-based model parameters and verify model output. Improved terrain representation has helped characterize hysteretic relationships between water storage and contributing area in large wetland complexes within parameterized runoff models (Shook et al., 2013), improve mapping in and along river channels to parameterize network level structure and flood inundation models (French, 2003; Kinzel et al., 2007; Snyder, 2009; Bates 2012), and expanded investigation of geomorphological change in floodplains (Thoma et al., 2005; Jones et al., 2007). Lidar provides vertical information that permits the direct retrieval of forest attributes such as tree height and canopy structure (Hyypä et al., 2012; Vosselman and Maas, 2010) that can be used to model canopy volume (Palminteri et al., 2012), biomass (Zhao et al., 2009), and the transmittance of solar radiation (Essery et al., 2008; Musselman et al., 2013; Bode et al., 2014). Lidar has also proven to be instrumental in the verification of model states. For example, lidar datasets have been used to verify physically-based models, including landscape evolution models (Pelletier et al., 2014; Pelletier and Perron, 2012; Rengers and Tucker, 2014), aeolian models (Pelletier et al., 2012; Pelletier, 2013), physiological models (Coops et al., 2013), snowpack energy balance models (Essery et al. 2008, Broxton et al., 2015), and an ecosystem dynamics model (Antonarakis et al., 2014). Simpler, empirical models have also been developed using lidar-derived estimates of soil erosion (Pelletier and Orem, 2014) and snow accumulation and ablation (Varhola et al., 2014). Better recognition of the potential benefits of lidar for model calibration and verification within CZ modeling community could lead to increased utilization and targeted acquisitions in the future.

368

369 **2.3 Adoption and Utilization of Lidar Datasets**

370 New and improved lidar datasets are more likely to result in transformative CZ science if a
371 number of key opportunities (and impediments) are recognized. The research topics discussed in
372 Section 2.2 require attention to four key areas in order to maximize the applicability of lidar in
373 CZ science: 1) Emerging data acquisition technology, 2) Availability of processing and analysis
374 techniques, 3) Linkages to *in situ* observations, and 4) Linkages to other remote sensing
375 observations. The first two areas recognize the importance of technological advances and
376 information sharing to enhance lidar data quality and coverage. The second two areas
377 demonstrate the potential to extend scientific inferences made from lidar with linkages to
378 multiple, complementary observations.

379

380 **2.3.1 Data Acquisition Technology**

381 Future advances in data acquisition technologies will provide greater information and
382 spatiotemporal coverage from lidar (and lidar-like) datasets. Several new lidar technologies are
383 rapidly increasing data quality (accuracy, precision, resolution, etc.) and information content.
384 Full waveform lidar data promises to provide better definition of ground surface and vegetation
385 canopy (Wagner et al, 2008, Mallet and Bretar, 2009). Utilizing blue-green light spectrum, lidar
386 systems are capable of bathymetric profiling (McKean et al., 2009; Fernandez-Diaz et al., 2014)
387 and potentially determining turbidity and inherent optical properties of the water column. Lidar
388 systems have demonstrated the benefits of combining point clouds with alternative data sources
389 by, for example, including intensity and/or RGB cameras (Bork and Su, 2007) that collect data
390 synchronously with the lidar and provide metadata for each point in the cloud. Less expensive

391 and more adaptable lidar systems (Brooks et al, 2013) and alternative 3-D remote sensing
392 techniques, such as SfM or low-cost 3D cameras (Mankoff and Russo, 2013; Javernick et al.,
393 2014; Lam et al., 2015), promise high resolution monitoring at finer temporal resolutions and
394 lower costs. Increasingly, lidar observations are combined with passive electro-optical
395 multispectral and hyperspectral images (Kurz et al., 2011). Lidar technology already includes
396 active multispectral laser systems, and hyperspectral laser observations of object reflectance are
397 likely only three to five years away (Hakala et al, 2012; Hartzell et al., 2014). These systems
398 promise to lessen the need for multiple sensors, thus reducing uncertainties due to data
399 registration, lowering costs, and reducing processing time. The combination of these
400 technologies holds promise as a means to cost-effectively monitor aspects of the CZ at time
401 scales of days or less, with information content that includes not only 3D structure, but also
402 spectral information that is potentially capable of determining vegetation composition and health,
403 soil and exposed bedrock composition, and soil water content.

404

405 In addition to emerging lidar acquisition systems, new and existing collection platforms are
406 substantially broadening data coverage. Collection of lidar from fixed-wing aircraft is expanding
407 to national scales through programs such as the U.S. Geological Survey's 3-D Elevation Program
408 (3DEP), Switzerland's national lidar dataset collected by the Federal Office of Topography,
409 Sweden's Lantmateriet (<http://www.lantmateriet.se>), Netherlands' Public Map Service
410 (<http://www.pdok.nl/en/node>), Denmark's Geodata Agency (<http://gst.dk>), Finland's National
411 Land Survey (<http://www.maanmittauslaitos.fi/en/maps-5>), United Kingdom's Environment
412 Agency (<http://www.geomatics-group.co.uk/GeoCMS>), and Australia's AusCover
413 (<http://www.auscover.org.au/>). Additionally, acquisition of aircraft and lidar systems by

414 institutional research programs have led to greater capabilities for ecological research by the
415 National Ecological Observatory Network (Kampe et al., 2010) and snow water resources via
416 NASA's Airborne Snow Observatory (<http://aso.jpl.nasa.gov>). Institutional systems and
417 operational expertise are also available for short-term research projects across a range of Earth
418 science applications (Glennie et al., 2013) by the National Center for Airborne Laser Mapping
419 (NCALM) and UNAVCO. Of particular interest to the CZ community is the development of
420 unmanned aerial systems (UASs) that are capable of mounting small lidar systems for rapid
421 deployment (Lin et al., 2011; Wallace et al., 2012). Long-range UASs offer the potential for
422 repeat lidar acquisitions at a fraction of the cost of current ALS platforms. Best practices for
423 collecting, processing and analyzing lidar over increasing extents (i.e. continental scales) are
424 generally lacking, which can limit the effectiveness of datasets collected over vastly different
425 physiographic conditions.

426

427 ***2.3.2 Data Access, Processing, and Analysis***

428 The crux in successfully leveraging a flood of new lidar (and other high-resolution topographic
429 information) data for CZ science (e.g. Stennett, 2004) will be the ability to extract meaningful
430 information from these rich and voluminous datasets. These new lidar datasets require data
431 processing and analysis tools be optimized to handle increasingly large datasets with greater
432 information content. Processing limitations are likely to reduce the usability and extent of very
433 high information datasets, e.g. waveform or multispectral datasets pose processing challenges at
434 the continental scale that may be more manageable at the watershed scale. Further, new software
435 and workflows need to be developed that enable scientists to incorporate lidar data into detailed
436 models of the CZ without expertise in remote sensing. The CZ science community must engage

437 in a concerted effort to develop (and/or adopt from other domains) new open source tools that
438 leverage high performance computing resources available through programs such as NSF's
439 XSEDE (<https://www.xsede.org/home>). By increasing the scalability of CZ lidar-oriented
440 processing and analysis tools, computationally intensive analysis and modeling at the highest
441 resolution of the lidar datasets will be possible. In addition to increasing software scalability,
442 new processing tools are necessary to take advantage of new data types, such as full waveform
443 lidar (Wagner et al, 2008, Mallet and Bretar, 2009) and hyperspectral laser technology (Hakala et
444 al, 2012). Cloud computing and the 'big data paradigm' that is increasingly common in both
445 industry and academia (Mattman, 2013) present opportunities for the CZ lidar community. One
446 such opportunity for big data sharing is EarthCube (www.earthcube.org), a relatively new
447 program that has potential to integrate lidar information (among other geospatial information)
448 into data sharing efforts in the geosciences. Due to efforts such as NSF's OpenTopography
449 (Crosby et al., 2011), there is a large volume of CZ-oriented lidar online and feely available to
450 the community. For example from the U.S., OpenTopography already offers on-demand
451 processing services (Krishnan et al., 2011) that permit users to generate standard and commonly
452 used derivatives from the hosted lidar point cloud. By coupling data processing with data access,
453 users are not required to download large volumes of data locally or have the dedicated
454 computing and software resources to process these data. Although many CZ-oriented lidar
455 datasets are already available to the community through resources such as OpenTopography in
456 the U.S., there are numerous other lidar datasets globally that are not accessible because they are
457 not available online or access is restricted. Many of these 'legacy' datasets are likely to be
458 important temporal baselines for comparison against future data focused on understanding CZ
459 processes (Glennie et al., 2014; Harpold et al., 2014a).

460

461 **2.3.3 Linkages To In Situ Observations**

462 Many CZ studies have incorporated *in situ* observations to extend or confirm inferences made
463 with lidar-derived datasets. *In situ* measurements are time consuming to collect, often expensive
464 to analyze, and limited in terms of spatial coverage. As a result, researchers must be judicious
465 with *in situ* data collection and maximize integration with lidar datasets. Physical and chemical
466 properties of soil and rock, and vegetation structure are among the *in situ* observations
467 commonly integrated with lidar datasets. For example, lidar-based studies have integrated
468 distributed measurements of soil hydraulic properties (Harman et al., 2014) and soil thickness
469 (Roering et al., 2010; Pelletier et al., 2014; West et al 2014), as well as radioactive isotopes in
470 soils (West et al., 2014). Lidar datasets have also been used to extend *in situ* observations of
471 snow depth (Harpold et al., 2014a; Varhola and Coops, 2013) and carbon fluxes (Hudak et al.,
472 2012) in both space and time. *In situ* observations of vegetation structural characteristics are
473 commonly made to develop relationships with lidar observations and extend these relationships
474 for forest inventory (e.g. Wulder et al., 2002). In addition to scientific inferences, lidar can be
475 used to improve sampling design to reduce time and analytical expenses. For example, lidar has
476 improved insight into sampling snow measurements necessary for water management
477 (McCreight et al., 2014). A number of challenges remain to link lidar-derived information to *in*
478 *situ* measurements, including poor GPS information for historical datasets, constraining the
479 observational footprint of different measurements, and comparing lidar-derived metrics to typical
480 field measurements. Despite these challenges, opportunities exist to better integrate historical
481 measurements into lidar-based studies and develop new *in situ* observations that use lidar
482 datasets to up-scale CZ processes.

483

484 **2.3.4 Linkages to Satellite Remote Sensing**

485 Satellite observations of surface-altimetry, reflectance, permittivity, and atmospheric profiles
486 provide observations of CZ processes at multiple spatiotemporal scales, frequently with global
487 coverage. The high spatial resolution offered by lidar technology complements the regular
488 temporal frequency of optical and radar satellite observations, which could be used to co-
489 calibrate and co-validate these types of datasets. Satellites also provide another platform for lidar
490 acquisition. There are numerous examples where lidar datasets have been used to calibrate and
491 verify coarser estimates of vegetation, cryosphere (e.g. glaciers, permafrost, snowpacks, etc.),
492 and geomorphic processes and states made via optical and radar satellites. For example, Mora et
493 al. (2013) used detailed lidar measurements of vegetation structure to quantify the spatial and
494 temporal scalability of above ground biomass of continental forests measured with the very high
495 spatial resolution (VHSR) satellite. In data-limited regions of Uganda, lidar fused with Landsat
496 datasets have improved modeled biomass predictions and understanding of phenologic processes
497 (Avitable et al., 2012). Varhola and Coops (2013) and Ahmed et al. (2014) introduce methods
498 for detecting changes in vegetation structure and function from disturbance by fusing Landsat
499 and lidar measurements, and Bright et al. (2014) used similar fused datasets to investigate
500 changes following forest mortality. Applications combining lidar and satellite measurements to
501 change detection have also been applied to evaluate the effects of vegetation on snowpack
502 dynamics (Varhola et al., 2014) and for comparison with model and satellite-derived estimates of
503 snow-covered area (Kirchner et al., 2014; Hedrick et al., 2014). A multifaceted approach for the
504 prediction and monitoring of landslides was proposed by Guzzeti (2012) using measurements
505 from optical satellites and lidar. The Ice, Cloud, and land Elevation Satellite (ICESat) was a

506 NASA mission from 2003 to 2009 that mapped changes in glacier mass balance using SLS
507 (Kohler et. al. 2013). Scientists have used ICESat’s Geoscience Laser Altimeter System (GLAS)
508 to identify areas of forest regeneration along the Mississippi (Li et al., 2011) and it has been
509 applied in development of a global forest height map (Simard et al., 2011). A second mission
510 (ICESat-2) is slated to launch in 2017 and while focused on ice sheet and sea ice change, it will
511 provide complementary products to characterize terrestrial ecology. Furthermore, other current
512 and future satellite missions will provide CZ observations that integrate with lidar, including soil
513 moisture, groundwater storage, soil freeze/thaw, carbon flux, and primary productivity (Schimel
514 et. al. 2013). Of particular interest might be the Surface Water and Ocean Topography (SWOT)
515 mission that provides coarse water and land topography using radar that has potential to
516 complement finer-scale measurements acquired with lidar. To fully realize the potential
517 information available from fused lidar and satellite datasets, critical attention must be paid to 1)
518 efficient processing of large datasets that span collection platforms and spatiotemporal variability,
519 and 2) maintaining expert knowledge in data interpretation (Matmann, 2013).

520

521 **2.4 A Proposed Five-Year Vision**

522 The fields of CZ science and lidar-based technology are both advancing rapidly. Here, we
523 present a vision that recognizes advances in science and technology to best position CZ
524 researchers at the forefront of the lidar revolution, particularly with regards to new hardware,
525 processing capabilities, and linkages with complementary observations. These ideas are guided
526 by the recognition that lidar is capable of simultaneously observing process signatures from
527 multiple CZ disciplines (Figure 1). To elucidate this point, we discuss three examples of
528 transdisciplinary CZ research questions and suggest how they could benefit from current and

529 future lidar technologies. We also provide specific recommendations for CZ researchers working
530 (or considering working) with lidar datasets. Our intent is to catalyze CZ interest in the
531 transdisciplinary possibilities of lidar datasets, while increasing the influence of CZ scientists
532 within the broader group of lidar end-users.

533

534 Technological advances can be conceptualized as increasing data coverage, quality, and
535 information, including new acquisition platforms or higher acquisition rates (Figure 3). Other
536 advances, such as full-waveform information or hyperspectral lasers, will increase the data
537 quality and information content extractable from lidar datasets. Some examples of linked
538 transdisciplinary research questions (Figure 3) that demonstrate the value of technological
539 advances in lidar for CZ science are, 1) How does co-variation between vegetation and
540 hydrological flowpaths control the likelihood and distribution of earth flows and landslides? 2)
541 How is the rapidly changing cryosphere influencing hydrological connectivity, drainage network
542 organization, nutrient and sediment fluxes, land-surface energy inputs, and vegetation structure?
543 3) How does above- and below-ground biomass control bedrock to soil production rates,
544 sediment mixing and transport and associated carbon fluxes via bioturbation and hillslope
545 transport? These example questions demonstrate the need for research that transcends
546 information sharing across disciplines to develop synergistic new theories and advances in CZ
547 science.

548

549 These research questions span a wide-range of spatial and temporal scales, from smaller and
550 faster (10^{-2} m and 10^1 s) in Question 3 to larger and more long-term (10^5 m and 10^6 s) in
551 Question 2 (see Figure 1). Our ability to answer these questions benefits from several facets of

552 improving lidar technologies, including higher acquisition rates and larger ranges, more rapid
553 and robust deployment options, and improved processing resources for extracting information.
554 Future lidar technologies could address Question 1 by identifying specific vegetation species via
555 hyperspectral laser technologies, increasing accuracy of bare-earth estimation to improve
556 hydrologic routing using full waveform analysis, and increasing coverage of landslide-prone
557 areas from different physiographic regions (Figure 3). New technology will address Question 2
558 by providing estimates of riparian vegetation productivity, measuring channel bathymetry using
559 blue-green lidar, and with new platforms that increase sampling frequency via UASs or other
560 low cost systems. Lastly, new technology will address Question 3 by providing improved
561 estimates of above-ground biomass and bare-earth extraction using full waveform analysis, and
562 improved fine-scale change detection with greater processing resources. The goal of these
563 example questions and their conceptualization (Figure 3) is to provide the reader with concrete
564 examples of what well-integrated lidar datasets can provide to stimulate and improve future CZ
565 research.

566

567 We propose five recommendations as an attempt to unite the CZ community around improved
568 utilization and advocacy of lidar technology in important transdisciplinary scientific contexts that
569 integrate the opportunities and impediments discussed previously:

570 · **Open lines of communication:** Develop communication within and among groups,
571 including individual CZ disciplines, remote sensing scientists, computer scientists, private
572 industry, and funding agencies. Workshops have the potential to increase communication
573 between ‘data-users’ and ‘data-creators’. CZ scientists must find ways to communicate their data
574 acquisition specifications to the scientists and engineers who create lidar hardware and

575 processing software through venues such as meetings with private industry, the development of
576 advisory committees, and commentary pieces in trade journals that present a vision for the future
577 needs of CZ scientists. Open communication among diverse CZ scientists is fundamental to
578 developing collaborations capable of transdisciplinary advances. Working groups within CZ
579 communities, like the critical zone exploration network (www.czen.org), and townhall meetings
580 at international Earth science conferences have initiated sustainable communication venues.
581 Future efforts focused on early-career CZ scientists that demonstrate the benefits of
582 transdisciplinary efforts, such as focused conferences and pilot research projects, should be
583 pursued.

584 · **Increase information extraction:** Advocate for lidar repositories that are interoperable
585 and broaden data access, as well as open-source and community-centric processing resources.
586 Ultimately, enhanced and streamlined data processing and analysis will enable CZ researchers to
587 concentrate on understanding fundamental science problems instead of struggling with data
588 access, processing, and analysis. Specifically, recent efforts focused on cloud storage and
589 computing resources, and open source software tools could greatly aid this effort. Efforts to
590 improve the efficiency of processing will become more important as the acquisition of lidar
591 expands to continental scales. Information extraction at larger extents will require judicious
592 tradeoffs between acquisition parameters and costs that consider variability in local
593 physiographic conditions (i.e. higher sampling densities in areas with dense vegetation cover and
594 high topographic complexity). Programs to support open source software and their long-term
595 sustainability are required to support CZ science. Increasing open access to lidar datasets
596 facilitates greater information extraction and the potential for meta-analysis studies. The value of
597 open-access datasets will increase as improved processing tools become available. CZ scientists

598 should also consider working with private lidar acquisition companies and their customers (i.e.
599 forestry, mining, and urban planning organizations) to release what has previously been
600 proprietary data to the public.

601 · **Increase accessibility of lidar systems:** Advocate for new acquisition technologies that
602 lower the cost of lidar collection and increase its availability, such as unmanned platforms and
603 less expensive and longer-range lidar systems. Institutional acquisitions of lidar systems also
604 significantly increase accessibility. Community-supported lidar systems available to researchers,
605 through agencies, such as UNAVCO and NCALM, should also be encouraged. A powerful
606 advancement would be a ‘clearinghouse’ where agencies and institutions could exchange
607 information on lidar systems, seek expert advice on lidar acquisition, and potentially trade or rent
608 hardware to better meet the needs of individual projects.

609 · **Focus on key technologies:** Support the development of new lidar technologies that are
610 useful for linking disciplinary observations. For example, our review has stressed the potential
611 benefits for linking CZ functions to processes offered by hyperspectral laser technologies (Figure
612 3). Other key technologies include new acquisition platforms (UASs) and improved open-source
613 processing capabilities and open-source industry-standard data formats. The community should
614 continue a dialogue about critical technologies within CZ science venues in parallel with
615 interactions with technology developers (as mentioned previously). The more united the CZ
616 community is about the benefits of a particular technology (i.e. hyperspectral lidar) the more it
617 can advocate within public and private sectors for its advancement.

618 · **Link complementary observations:** Consider other remote sensing observations that
619 may be complementary to lidar (e.g. thermal, infrared, optical, and microwave). While fusing
620 remote sensing data is becoming more common, the value of lidar information to coarser remote

621 sensing products is vast and underutilized. Be mindful of the potential synergistic benefits of
622 collecting lidar data over areas with *in situ* observations and vice versa, consider how to improve
623 collection of *in situ* observations based on lidar information. In particular, *in situ* information
624 collected during lidar data collection can be extremely valuable and difficult to substitute for at a
625 later date. Maintain awareness of competing, less expensive technologies, such as SfM, that may
626 be more appropriate in some conditions and geographical locations. The multi-scale nature of
627 transdisciplinary research (Figure 1 and 3) demands that lidar be integrated into a broader
628 observational framework that does not neglect the value of *in situ* and coarser remote sensing
629 observations.

630

631 **Acknowledgements:**

632 The workshop forming the impetus for this paper was funded by the National Science
633 Foundation (EAR 1406031). Additional funding for the workshop and planning was provided to
634 S.W. Lyon by the Swedish Foundation for International Cooperation in Research and Higher
635 Education (STINT Grant No. 2013-5261). A.A. Harpold was supported by an NSF fellowship
636 (EAR 1144894). The use of specific commercial or open-source packages and tools in this paper
637 does not imply a specific endorsement.

638

639

640 **References:**

- 641 Abdalati, W., H.J. Zwally, R. Bindenschadler, B. Csatho, S.L. Farrell, H.A. Fricker, D. Harding, R.
642 Kwok, M. Lefsky, T. Markus, A. Marshak, T. Neumann, S. Palm, B. Schutz, B. Smith, J.
643 Spinhirne, and C. Webb (2010), The ICESat-2 laser altimetry mission. *Proceedings of the*
644 *IEEE*, 98(5), 735-751, doi: 10.1109/JPROC.2009.2034765
- 645 Ahmed, O. S., S. E. Franklin, and M. A. Wulder (2014), Interpretation of forest disturbance
646 using a time series of Landsat imagery and canopy structure from airborne LiDAR,
647 *Canadian Journal of Remote Sensing*, 39(6), 521–542, doi:10.5589/m14-004.
- 648 Anderson, S., and J. Pitlick (2014), Using repeat LiDAR to estimate sediment transport in a steep
649 stream, *J. Geophys. Res. Earth Surf.*, 119(3), 621–643, doi:10.1002/2013JF002933.
- 650 Antonarakis, A. S., J. W. Munger, and P. R. Moorcroft (2014), Imaging spectroscopy- and
651 LiDAR-derived estimates of canopy composition and structure to improve predictions of
652 forest carbon fluxes and ecosystem dynamics, *Geophysical Research Letters*, 41(7),
653 2013GL058373, doi:10.1002/2013GL058373.
- 654 Antonarakis, A. S., K. S. Richards, J. Brasington, and E. Muller (2010), Determining leaf area
655 index and leafy tree roughness using terrestrial laser scanning, *Water Resources Research*,
656 46(6), W06510, doi:10.1029/2009WR008318.
- 657 Arnold, N. S., W. G. Rees, B. J. Devereux, and G. S. Amable (2006), Evaluating the potential of
658 high-resolution airborne LiDAR data in glaciology, *International Journal of Remote*
659 *Sensing*, 27(6), 1233–1251, doi:10.1080/01431160500353817.
- 660 Aryal, A., B. A. Brooks, M. E. Reid, G. W. Bawden, and G. R. Pawlak (2012), Displacement
661 fields from point cloud data: Application of particle imaging velocimetry to landslide
662 geodesy, *Journal of Geophysical Research: Atmospheres (1984–2012)*, 117(F1), F01029,
663 doi:10.1029/2011JF002161.
- 664 Asner, G. P., D. E. Knapp, J. Boardman, R. O. Green, T. Kennedy-Bowdoin, M. Eastwood, R. E.
665 Martin, C. Anderson, and C. B. Field (2012a), Carnegie Airborne Observatory-2: Increasing
666 science data dimensionality via high-fidelity multi-sensor fusion, *Remote Sensing of*
667 *Environment*, 124(0), 454–465, doi:10.1016/j.rse.2012.06.012.
- 668 Asner, G., J. Mascaro, H. Muller-Landau, G. Vieilledent, R. Vaudry, M. Rasamoelina, J. Hall,
669 and M. van Breugel (2012b), A universal airborne LiDAR approach for tropical forest
670 carbon mapping, *Oecologia*, 168(4), 1147–1160, doi:10.1007/s00442-011-2165-z.

671 Avitabile, V., A. Baccini, M. A. Friedl, and C. Schmullius (2012), Capabilities and limitations of
672 Landsat and land cover data for aboveground woody biomass estimation of Uganda, *Remote*
673 *Sensing of Environment*, 117(0), 366–380, doi:10.1016/j.rse.2011.10.012.

674 Baccini, A. et al. (2012), Estimated carbon dioxide emissions from tropical deforestation
675 improved by carbon-density maps, *Nature Climate change*, 2(3), 182–185,
676 doi:10.1038/nclimate1354.

677 Barnhart, T. B., and B. T. Crosby (2013), Comparing Two Methods of Surface Change Detection
678 on an Evolving Thermokarst Using High-Temporal-Frequency Terrestrial Laser Scanning,
679 Selawik River, Alaska, *Remote Sensing*, 5(6), 2813–2837, doi:10.3390/rs5062813.

680 Bates, P. D. (2012), Integrating remote sensing data with flood inundation models: how far have
681 we got? *Hydrol. Process.*, 26(16), 2515–2521, doi:10.1002/hyp.9374.

682 Belmont, P. et al. (2011), Large Shift in Source of Fine Sediment in the Upper Mississippi River,
683 *Environ. Sci. Technol.*, 45(20), 8804–8810, doi:10.1021/es2019109.

684 Bittner, S., S. Gayler, C. Biernath, J. B. Winkler, S. Seifert, H. Pretzsch, and E. Priesack (2014),
685 Evaluation of a ray-tracing canopy light model based on terrestrial laser scans, *Canadian*
686 *Journal of Remote Sensing*, 38(5), 619–628, doi:10.5589/m12-050.

687 Bode, C. A., M. P. Limm, M. E. Power, and J. C. Finlay (2014), Subcanopy Solar Radiation
688 model: Predicting solar radiation across a heavily vegetated landscape using LiDAR and GIS
689 solar radiation models, *Remote Sensing of Environment*, (0 SP - EP - PY - T2 -),
690 doi:10.1016/j.rse.2014.01.028.

691 Booth, A. M., J. J. Roering, and J. T. Perron (2009), Automated landslide mapping using spectral
692 analysis and high-resolution topographic data: Puget Sound lowlands, Washington, and
693 Portland Hills, Oregon, *Geomorphology*, 109(3-4), 132–147,
694 doi:10.1016/j.geomorph.2009.02.027.

695 Bork, E. W., and J. G. Su (2007), Integrating LIDAR data and multispectral imagery for
696 enhanced classification of rangeland vegetation: A meta analysis, *Remote Sensing of*
697 *Environment*, 111(1), 11–24, doi:10.1016/j.rse.2007.03.011.

698 Boutet, J., Jr, and J. Weishampel (2003), Spatial pattern analysis of pre- and post-hurricane forest
699 canopy structure in North Carolina, USA, *Landscape Ecology*, 18(6), 553–559,
700 doi:10.1023/A%3A1026058312853.

701 Brasington, J., D. Vericat, and I. Rychkov (2012), Modeling river bed morphology, roughness,

702 and surface sedimentology using high resolution terrestrial laser scanning, *Water Resources*
703 *Research*, 48(11), W11519, doi:10.1029/2012WR012223.

704 Bright, B. C., A. T. Hudak, R. McGaughey, H.-E. Andersen, and J. Negrón (2014), Predicting
705 live and dead tree basal area of bark beetle affected forests from discrete-return LiDAR,
706 *Canadian Journal of Remote Sensing*, 39(sup1), S99–S111, doi:10.5589/m13-027.

707 Brooks, B. A., C. Glennie, K. W. Hudnut, T. Ericksen, and D. Hauser (2013), Mobile Laser
708 Scanning Applied to the Earth Sciences, *Eos, Transactions American Geophysical Union*,
709 94(36), 313–315, doi:10.1002/2013EO360002.

710 Broxton, P. D., A. A. Harpold, P. D. Brooks, P. A. Troch, and N. P. Molotch (In Press),
711 Quantifying the effects of vegetation structure on wintertime vapor losses from snow in
712 mixed-conifer forests, *Ecohydrol*.

713 Brubaker, K. M., W. L. Myers, P. J. Drohan, D. A. Miller, and E. W. Boyer (2013), The Use of
714 LiDAR Terrain Data in Characterizing Surface Roughness and Microtopography, *Applied*
715 *and Environmental Soil Science*, 2013, 13, doi:10.1155/2013/891534.

716 Cho, M. A. et al. (2012), Mapping tree species composition in South African savannas using an
717 integrated airborne spectral and LiDAR system, *Remote Sensing of Environment*, 125(0),
718 214–226, doi:10.1016/j.rse.2012.07.010.

719 Chorover, J. et al. (2011), How Water, Carbon, and Energy Drive Critical Zone Evolution: The
720 Jemez–Santa Catalina Critical Zone Observatory, *Vadose Zone Journal*, 10(3), 884–899.

721 Coops, N. C., F. Morsdorf, M. E. Schaepman, and N. E. Zimmermann (2013), Characterization
722 of an alpine tree line using airborne LiDAR data and physiological modeling, *Global*
723 *Change Biology*, 19(12), 3808–3821, doi:10.1111/gcb.12319.

724 Crosby, C., R. Arrowsmith, V. Nandigam, and C. Baru (2011), Online access and processing of
725 LiDAR topography data, edited by G. R. Keller and C. Baru, Cambridge University Press.

726 Day, S. S., K. B. Gran, P. Belmont, and T. Wawrzyniec (2013), Measuring bluff erosion part 1:
727 terrestrial laser scanning methods for change detection, *Earth Surface Processes and*
728 *Landforms*, 38(10), 1055–1067, doi:10.1002/esp.3353.

729 Deems, J. S., S. R. Fassnacht, and K. J. Elder (2006), Fractal Distribution of Snow Depth from
730 LiDAR Data, *J. Hydrometeor*, 7(2), 285–297, doi:10.1175/JHM487.1.

731 Deems, J. S., S. R. Fassnacht, and K. J. Elder (2008), Interannual Consistency in Fractal Snow
732 Depth Patterns at Two Colorado Mountain Sites, *J. Hydrometeor*, 9(5), 977–988,

733 doi:10.1175/2008JHM901.1.

734 Deems, J. S., T. H. Painter, and D.C. Finnegan (2013), LiDAR measurement of snow depth: a
735 review, *Journal of Glaciology*, 59(215), 467-479, doi.org/10.3189/2013JoG12J154

736 DeLong, S. B., C. S. Prentice, G. E. Hilley, and Y. Ebert (2012), Multitemporal ALSM change
737 detection, sediment delivery, and process mapping at an active earthflow, *Earth Surface*
738 *Processes and Landforms*, 37(3), 262–272, doi:10.1002/esp.2234.

739 Dickinson, Y., E. K. Zenner, and D. Miller (2014), Examining the effect of diverse management
740 strategies on landscape scale patterns of forest structure in Pennsylvania using novel remote
741 sensing techniques, *Can. J. For. Res.*, 44(4), 301–312, doi:10.1139/cjfr-2013-0315.

742 Drake, J. B., and J. F. Weishampel (2000), Multifractal analysis of canopy height measures in a
743 longleaf pine savanna, *Forest Ecology and Management*, 128(1–2), 121–127,
744 doi:10.1016/S0378-1127(99)00279-0.

745 Egli, L., T. Jonas, T. Grünewald, M. Schirmer, and P. Burlando (2012), Dynamics of snow
746 ablation in a small Alpine catchment observed by repeated terrestrial laser scans, *Hydrol.*
747 *Process.*, 26(10), 1574–1585, doi:10.1002/hyp.8244.

748 Essery, R., P. Bunting, A. Rowlands, N. Rutter, J. Hardy, R. Melloh, T. Link, D. Marks, and J.
749 Pomeroy (2008), Radiative Transfer Modeling of a Coniferous Canopy Characterized by
750 Airborne Remote Sensing, *J. Hydrometeor.*, 9(2), 228–241, doi:10.1175/2007JHM870.1.

751 Fassnacht, S. R., and J. S. Deems (2006), Measurement sampling and scaling for deep montane
752 snow depth data, *Hydrol. Process.*, 20(4), 829–838, doi:10.1002/hyp.6119.

753 Fernandez-Diaz, J. C., C. L. Glennie, W. E. Carter, R. L. Shrestha, M. P. Sartori, A. Singhanian,
754 C. J. Legleiter, and B. T. Overstreet (2014), Early Results of Simultaneous Terrain and
755 Shallow Water Bathymetry Mapping Using a Single-Wavelength Airborne LiDAR Sensor,
756 *Selected Topics in Applied Earth Observations and Remote Sensing, IEEE Journal of*, 7(2),
757 623–635, doi:10.1109/JSTARS.2013.2265255.

758 Fewtrell, T. J., P. D. Bates, M. Horritt, and N. M. Hunter (2008), Evaluating the effect of scale in
759 flood inundation modelling in urban environments, *Hydrol. Process.*, 22(26), 5107–5118,
760 doi:10.1002/hyp.7148.

761 Féret, J.-B., and G. P. Asner (2012), Semi-Supervised Methods to Identify Individual Crowns of
762 Lowland Tropical Canopy Species Using Imaging Spectroscopy and LiDAR, *Remote*
763 *Sensing*, 4(8), 2457–2476, doi:10.3390/rs4082457.

764 Flener, C., M. Vaaja, A. Jaakkola, A. Krooks, H. Kaartinen, A. Kukko, E. Kasvi, H. Hyypä, J.
765 Hyypä, and P. Alho (2013), Seamless Mapping of River Channels at High Resolution
766 Using Mobile LiDAR and UAV-Photography, *Remote Sensing*, 5(12), 6382–6407,
767 doi:10.3390/rs5126382.

768 Fonstad, M. A., J.T. Dietrich, B.C. Courville, J.L Jensen, and P.E. Carbonneau (2013).
769 Topographic structure from motion: a new development in photogrammetric measurement,
770 *Earth Surface Processes and Landforms*, 38(4), 421-430, doi: 10.1002/esp.3366.

771 Forzieri, G., G. Moser, E. R. Vivoni, F. Castelli, and F. Canovaro (2010), Riparian Vegetation
772 Mapping for Hydraulic Roughness Estimation Using Very High Resolution Remote Sensing
773 Data Fusion, *Journal of Hydraulic Engineering*, 136(11), 855–867,
774 doi:10.1061/(ASCE)HY.1943-7900.0000254.

775 Frazer, G. W., M. A. Wulder, and K. O. Niemann (2005), Simulation and quantification of the
776 fine-scale spatial pattern and heterogeneity of forest canopy structure: A lacunarity-based
777 method designed for analysis of continuous canopy heights, *Forest Ecology and*
778 *Management*, 214(1–3), 65–90, doi:10.1016/j.foreco.2005.03.056.

779 French, J. R. (2003), Airborne LiDAR in support of geomorphological and hydraulic modelling,
780 *Earth Surface Processes and Landforms*, 28(3), 321–335, doi:10.1002/esp.484.

781 Glenn, N. F., D. R. Streutker, D. J. Chadwick, G. D. Thackray, and S. J. Dorsch (2006), Analysis
782 of LiDAR-derived topographic information for characterizing and differentiating landslide
783 morphology and activity, *Geomorphology*, 73(1–2), 131–148,
784 doi:10.1016/j.geomorph.2005.07.006.

785 Glennie, C. L., A. Hinojosa-Corona, E. Nissen, A. Kusari, M. E. Oskin, J. R. Arrowsmith, and A.
786 Borsa (2014), Optimization of legacy LiDAR data sets for measuring near-field earthquake
787 displacements, *Geophysical Research Letters*, 41(10), 2014GL059919,
788 doi:10.1002/2014GL059919.

789 Glennie, C. L., W. E. Carter, R. L. Shrestha, and W. E. Dietrich (2013), Geodetic imaging with
790 airborne LiDAR: the Earth's surface revealed, *Rep. Prog. Phys.*, 76(8), 086801.

791 Guzzetti, F., A. C. Mondini, M. Cardinali, F. Fiorucci, M. Santangelo, and K.-T. Chang (2012),
792 Landslide inventory maps: New tools for an old problem, *Earth Science Reviews*, 112(1–2),
793 42–66, doi:10.1016/j.earscirev.2012.02.001.

794 Grünewald, T., M. Schirmer, R. Mott, and M. Lehning (2010). Spatial and temporal variability

795 of snow depth and SWE in a small mountain catchment, *The Cryosphere*, 4, 215-230,
796 doi:10.5194/tc-4-215-2010

797 Hakala, T., J. Suomalainen, S. Kaasalainen, and Y. Chen (2012), Full waveform hyperspectral
798 LiDAR for terrestrial laser scanning, *Opt. Express*, 20(7), 7119–7127,
799 doi:10.1364/OE.20.007119.

800 Harman, C. J., K. A. Lohse, P. A. Troch, and M. Sivapalan (2014), Spatial patterns of vegetation,
801 soils, and microtopography from terrestrial laser scanning on two semiarid hillslopes of
802 contrasting lithology, *J. Geophys. Res. Biogeosci.*, 119(2), 163–180,
803 doi:10.1002/2013JG002507.

804 Harpold, A. A. et al. (2014a), LiDAR-derived snowpack data sets from mixed conifer forests
805 across the Western United States, *Water Resources Research*, 50(3), 2749–2755,
806 doi:10.1002/2013WR013935.

807 Harpold, A. A., J. A. Biederman, K. Condon, M. Merino, Y. Korgaonkar, T. Nan, L. L. Sloat, M.
808 Ross, and P. D. Brooks (2014b), Changes in snow accumulation and ablation following the
809 Las Conchas Forest Fire, New Mexico, USA, *Ecohydrol.*, 7(2), 440–452,
810 doi:10.1002/eco.1363.

811 Hartzell, P., C. Glennie, K. Biber, and S. Khan (2014), Application of multispectral LiDAR to
812 automated virtual outcrop geology, *ISPRS Journal of Photogrammetry and Remote Sensing*,
813 88(0), 147–155, doi:10.1016/j.isprsjprs.2013.12.004.

814 Hedrick, A., H. P. Marshall, A. Winstral, K. Elder, S. Yueh, and D. CLINE (2014), Independent
815 evaluation of the SNODAS snow depth product using regional scale LiDAR-derived
816 measurements, *The Cryosphere Discussions*, 8(3), 3141–3170, doi:10.5194/tcd-8-3141-
817 2014.

818 Hopkinson, C., and M. N. Demuth (2006), Using airborne LiDAR to assess the influence of
819 glacier downwasting on water resources in the Canadian Rocky Mountains, *Canadian*
820 *Journal of Remote Sensing*, 32(2), 212–222, doi:10.5589/m06-012.

821 Hopkinson, C., J. Lovell, L. Chasmer, D. Jupp, N. Kljun, and E. van Gorsel (2013), Integrating
822 terrestrial and airborne LiDAR to calibrate a 3D canopy model of effective leaf area index,
823 *Remote Sensing of Environment*, 136(0), 301–314, doi:10.1016/j.rse.2013.05.012.

824 Hopkinson, C., T. Collins, A. Anderson, J. Pomeroy, and I. Spooner (2012), Spatial Snow Depth
825 Assessment Using LiDAR Transect Samples and Public GIS Data Layers in the Elbow River

826 Watershed, Alberta, *Canadian Water Resources Journal*, 37(2), 69–87,
827 doi:10.4296/cwrj3702893.

828 Hudak, A. T., E. K. Strand, L. A. Vierling, J. C. Byrne, J. U. H. Eitel, S. Martinuzzi, and M. J.
829 Falkowski (2012), Quantifying aboveground forest carbon pools and fluxes from repeat
830 LiDAR surveys, *Remote Sensing of Environment*, 123(0), 25–40,
831 doi:10.1016/j.rse.2012.02.023.

832 Hurst, M. D., S. M. Mudd, K. Yoo, M. Attal, and R. Walcott (2013), Influence of lithology on
833 hillslope morphology and response to tectonic forcing in the northern Sierra Nevada of
834 California, *J. Geophys. Res. Earth Surf.*, 118(2), 832–851, doi:10.1002/jgrf.20049.

835 Hurst, M. D., S. M. Mudd, R. Walcott, M. Attal, and K. Yoo (2012), Using hilltop curvature to
836 derive the spatial distribution of erosion rates, *Journal of Geophysical Research:*
837 *Atmospheres (1984–2012)*, 117(F2), F02017, doi:10.1029/2011JF002057.

838 Hyde, P., R. Dubayah, B. Peterson, J. B. Blair, M. Hofton, C. Hunsaker, R. Knox, and W.
839 Walker (2005), Mapping forest structure for wildlife habitat analysis using waveform
840 LiDAR: Validation of montane ecosystems, *Remote Sensing of Environment*, 96(3–4), 427–
841 437, doi:10.1016/j.rse.2005.03.005.

842 Hyypä, J., M. Holopainen, and H. Olsson (2012), Laser Scanning in Forests, *Remote Sensing*,
843 4(10), 2919–2922, doi:10.3390/rs4102919.

844 James, L. A., M. B. Singer, S. Ghoshal, and M. Megison (2009), Historical channel changes in
845 the lower Yuba and Feather Rivers, California: Long-term effects of contrasting river-
846 management strategies, *Geological Society of America Special Papers*, 451, 57–81,
847 doi:10.1130/2009.2451(04).

848 James, L. A., M. E. Hodgson, S. Ghoshal, and M. M. Latiolais (2012), Geomorphic change
849 detection using historic maps and DEM differencing: The temporal dimension of geospatial
850 analysis, *Geomorphology*, 137(1), 181–198, doi:10.1016/j.geomorph.2010.10.039.

851 Javernick, L., J. Brasington, and B. Caruso (2014), Modeling the topography of shallow braided
852 rivers using Structure-from-Motion photogrammetry, *Geomorphology*, 213(0), 166–182,
853 doi:10.1016/j.geomorph.2014.01.006.

854 Jencso, K. G., B.L. McGlynn, M.N. Gooseff, S.M. Wondzell, K.E. Bencala, and L.A. Marshall
855 (2009), Hydrologic connectivity between landscapes and streams: Transferring reach-and
856 plot-scale understanding to the catchment scale, *Water Resources Research*, 45(4), doi:

857 10.1029/2008WR007225

858 Jones, A. F., P. A. Brewer, E. Johnstone, and M. G. Macklin (2007), High-resolution
859 interpretative geomorphological mapping of river valley environments using airborne
860 LiDAR data, *Earth Surface Processes and Landforms*, 32(10), 1574–1592,
861 doi:10.1002/esp.1505.

862 Kaasalainen, S., T. Lindroos, and J. Hyypä (2007), Toward Hyperspectral LiDAR:
863 Measurement of Spectral Backscatter Intensity With a Supercontinuum Laser Source,
864 *Geoscience and Remote Sensing Letters, IEEE*, 4(2), 211–215,
865 doi:10.1109/LGRS.2006.888848.

866 Kampe, T. U., B.R. Johnson, M. Kuester, and M. Keller (2010), NEON: the first continental-
867 scale ecological observatory with airborne remote sensing of vegetation canopy biochemistry
868 and structure. *Journal of Applied Remote Sensing*, 4(1), 043510-043510, doi:
869 10.1117/1.3361375

870 Khamsin, I., M. Zulkarnain, K. A. Razak, and S. Rizal (2014), Detection of tropical landslides
871 using airborne LiDAR data and multi imagery: A case study in Genting highland, Pahang,
872 *IOP Conference Series: Earth and Environmental Science*, 18(1), 012033.

873 Kessler, A. C., S. C. Gupta, H. A. S. Dolliver, and D. P. Thoma (2012), LiDAR Quantification of
874 Bank Erosion in Blue Earth County, Minnesota, *Journal of Environmental Quality*, 41(1),
875 197–207, doi:10.2134/jeq2011.0181.

876 Kinzel, P. J., C. J. Legleiter, and J. M. Nelson (2013), Mapping River Bathymetry With a Small
877 Footprint Green LiDAR: Applications and Challenges¹, *JAWRA Journal of the American*
878 *Water Resources Association*, 49(1), 183–204, doi:10.1111/jawr.12008.

879 Kinzel, P. J., C. W. Wright, J. M. Nelson, and A. R. Burman (2007), Evaluation of an
880 Experimental LiDAR for Surveying a Shallow, Braided, Sand-Bedded River, *Journal of*
881 *Hydraulic Engineering*, 133(7), 838–842, doi:10.1061/(ASCE)0733-9429(2007)133:7(838).

882 Kirchner, P. B., R. C. Bales, N. P. Molotch, J. Flanagan, and Q. Guo (2014), LiDAR
883 measurement of seasonal snow accumulation along an elevation gradient in the southern
884 Sierra Nevada, California, *Hydrol. Earth Syst. Sci. Discuss.*, 11(5), 5327–5365,
885 doi:10.5194/hessd-11-5327-2014.

886 Kohler, J., T. A. Neumann, J. W. Robbins, S. Tronstad, and G. Melland (2013), ICESat
887 Elevations in Antarctica Along the 2007-09 Norway-USA Traverse: Validation With

888 Ground-Based GPS, *Geoscience and Remote Sensing, IEEE Transactions on*, 51(3), 1578–
889 1587, doi:10.1109/TGRS.2012.2207963.

890 Krishnan, S., C. Crosby, V. Nandigam, M. Phan, C. Cowart, C. Baru, and R. Arrowsmith (2011),
891 OpenTopography: A Services Oriented Architecture for Community Access to LIDAR
892 Topography, pp. 7:1–7:8, ACM, New York, NY, USA.

893 Kurz, T. H., S. J. Buckley, J. A. Howell, and D. Schneider (2011), Integration of panoramic
894 hyperspectral imaging with terrestrial LiDAR data, *The Photogrammetric Record*, 26(134),
895 212–228, doi:10.1111/j.1477-9730.2011.00632.x.

896 Lague, D., N. Brodu, and J. Leroux (2013), Accurate 3D comparison of complex topography
897 with terrestrial laser scanner: Application to the Rangitikei canyon (N-Z), *ISPRS Journal of*
898 *Photogrammetry and Remote Sensing*, 82(0), 10–26, doi:10.1016/j.isprsjprs.2013.04.009.

899 Lam, N., M. Nathanson, N. Lundgren, R. Rehnström, and S.W. Lyon (2015), A Cost-Effective
900 Laser Scanning Method for Mapping Stream Channel Geometry and Roughness, *Journal*
901 *of the American Water Resources Association*, 1-10. DOI: 10.1111/1752-1688.12299.

902 Lane, S. N., C.J. Brookes, M.J. Kirkby, and J. Holden (2004), A network-index-based version of
903 TOPMODEL for use with high-resolution digital topographic data, *Hydrological*
904 *processes*, 18(1), 191-201, doi: 10.1002/hyp.5208.

905 Lane, C. R., and E. D’Amico (2010), Calculating the Ecosystem Service of Water Storage in
906 Isolated Wetlands using LiDAR in North Central Florida, USA, *Wetlands*, 30(5), 967–977,
907 doi:10.1007/s13157-010-0085-z.

908 Lee, H., K. C. Slatton, B. E. Roth, and W. P. Cropper (2009), Prediction of forest canopy light
909 interception using three-dimensional airborne LiDAR data, *International Journal of*
910 *Remote Sensing*, 30(1), 189–207, doi:10.1080/01431160802261171.

911 Lefsky, M. A., W. B. Cohen, G. G. Parker, and D. J. Harding (2002), Remote Sensing for
912 Ecosystem Studies: LiDAR, an emerging remote sensing technology that directly measures
913 the three-dimensional distribution of plant canopies, can accurately estimate vegetation
914 structural attributes and should be of particular interest to forest, landscape, and global
915 ecologists, *BioScience*, 52(1), 19–30, doi:10.1641/0006-
916 3568(2002)052[0019:LRSFES]2.0.CO.

917 Legleiter, C. J., P. C. Kyriakidis, R. R. McDonald, and J. M. Nelson (2011), Effects of uncertain
918 topographic input data on two-dimensional flow modeling in a gravel-bed river, *Water*

919 *Resources Research*, 47(3), W03518, doi:10.1029/2010WR009618.

920 Levy, J. S., A. G. Fountain, J. L. Dickson, J. W. Head, M. Okal, D. R. Marchant, and J. Watters
921 (2013), Accelerated thermokarst formation in the McMurdo Dry Valleys, Antarctica, *Sci.*
922 *Rep.*, 3, doi:10.1038/srep02269.

923 Li, S., R. A. MacMillan, D. A. Lobb, B. G. McConkey, A. Moulin, and W. R. Fraser (2011),
924 LiDAR DEM error analyses and topographic depression identification in a hummocky
925 landscape in the prairie region of Canada, *Geomorphology*, 129(3–4), 263–275,
926 doi:10.1016/j.geomorph.2011.02.020.

927 Lin, Y., J. Hyypä, and A. Jaakkola (2011), Mini-UAV-Borne LIDAR for Fine-Scale Mapping,
928 *Geoscience and Remote Sensing Letters, IEEE*, 8(3), 426–430,
929 doi:10.1109/LGRS.2010.2079913.

930 Liu, Z. et al. (2008), CALIPSO LiDAR observations of the optical properties of Saharan dust: A
931 case study of long-range transport, *Journal of Geophysical Research: Atmospheres (1984–*
932 *2012)*, 113(D7), D07207, doi:10.1029/2007JD008878.

933 Lotsari, E., M. Vaaja, C. Flener, H. Kaartinen, A. Kukko, E. Kasvi, H. Hyypä, J. Hyypä, and
934 P. Alho (2014), Annual bank and point bar morphodynamics of a meandering river
935 determined by high-accuracy multitemporal laser scanning and flow data, *Water Resources*
936 *Research*, 50, 5532–5559, doi:10.1002/2013WR014106.

937 Lyon, S.W., M. Nathanson, N. Lam, H.E. Dahlke, M. Rutzinger, J.W. Kean and H. Laudon
938 (2015), Can Low-Resolution Airborne Laser Scanning Data Be Used to Model Stream
939 Rating Curves?, *Water*, 7(4), 1324–1339, doi:10.3390/w7041324.

940 Mallet, C. and F. Bretar (2009). Full-waveform topographic LiDAR: State-of-the-art, *ISPRS*
941 *Journal of Photogrammetry and Remote Sensing*, 64(1), 1–16, doi:
942 10.1016/j.isprsjprs.2008.09.007.

943 Maltamo, M., E. Næsset, and J. Vauhkonen (Eds.) (2014), *Forestry Applications of Airborne*
944 *Laser Scanning*, Springer, Netherlands.

945 Mandlbürger, G., C. Hauer, B. Höfle, H. Habersack, N. Pfeifer, others (2009), Optimisation of
946 LiDAR derived terrain models for river flow modelling, *Hydrol. Earth Syst. Sci.*, 13(8),
947 1453–1466, doi:10.5194/hess-13-1453-2009.

948 Mankoff, K. D., and T. A. Russo (2013), The Kinect: a low-cost, high-resolution, short-range 3D
949 camera, *Earth Surface Processes and Landforms*, 38(9), 926–936, doi:10.1002/esp.3332.

950 Marks, K., and P. Bates (2000), Integration of high-resolution topographic data with floodplain
951 flow models, *Hydrol. Process.*, *14*(11-12), 2109–2122, doi:10.1002/1099-
952 1085(20000815/30)14:11/12<2109::AID-HYP58>3.0.CO;2-1.

953 Marshall, J. A., and J. J. Roering (2014), Diagenetic variation in the Oregon Coast Range:
954 Implications for rock strength, soil production, hillslope form, and landscape evolution, *J.*
955 *Geophys. Res. Earth Surf.*, *119*(6), 2013JF003004, doi:10.1002/2013JF003004.

956 Martinuzzi, S., L. A. Vierling, W. A. Gould, M. J. Falkowski, J. S. Evans, A. T. Hudak, and K.
957 T. Vierling (2009), Mapping snags and understory shrubs for a LiDAR-based assessment of
958 wildlife habitat suitability, *Remote Sensing of Environment*, *113*(12), 2533–2546,
959 doi:10.1016/j.rse.2009.07.002.

960 Mascaro, J., M. Detto, G. P. Asner, and H. C. Muller-Landau (2011), Evaluating uncertainty in
961 mapping forest carbon with airborne LiDAR, *Remote Sensing of Environment*, *115*(12),
962 3770–3774, doi:10.1016/j.rse.2011.07.019.

963 Mason, D. C., D. M. Cobby, M. S. Horritt, and P. D. Bates (2003), Floodplain friction
964 parameterization in two-dimensional river flood models using vegetation heights derived
965 from airborne scanning laser altimetry, *Hydrol. Process.*, *17*(9), 1711–1732,
966 doi:10.1002/hyp.1270.

967 Mattmann, C. A. (2013), Computing: A vision for data science, *Nature*, *493*(7433), 473-475,
968 doi:10.1038/493473a

969 McCreight, J. L., A. G. Slater, H. P. Marshall, and B. Rajagopalan (2014), Inference and
970 uncertainty of snow depth spatial distribution at the kilometre scale in the Colorado Rocky
971 Mountains: the effects of sample size, random sampling, predictor quality, and validation
972 procedures, *Hydrol. Process.*, *28*(3), 933–957, doi:10.1002/hyp.9618.

973 McKean, J. A., D. J. Isaak, and C. W. Wright (2008), Geomorphic controls on salmon nesting
974 patterns described by a new, narrow-beam terrestrial–aquatic LiDAR, *Frontiers in Ecology*
975 *and the Environment*, *6*(3), 125–130, doi:10.1890/070109.

976 McKean, J., D. Isaak, and W. Wright (2009), Improving stream studies with a small-footprint
977 green LiDAR, *Eos, Transactions American Geophysical Union*, *90*(39), 341–342,
978 doi:10.1029/2009EO390002.

979 McKean, J., D. Tonina, C. Bohn, and C. W. Wright (2014), Effects of bathymetric LiDAR errors
980 on flow properties predicted with a multi-dimensional hydraulic model, *J. Geophys. Res.*

981 *Earth Surf.*, 119(3), 2013JF002897, doi:10.1002/2013JF002897.

982 Meyer, V., S. S. Saatchi, J. Chave, J. Dalling, S. Bohlman, G. A. Fricker, C. Robinson, and M.
983 Neumann (2013), Detecting tropical forest biomass dynamics from repeated airborne LiDAR
984 measurements, *Biogeosciences Discussions*, 10(2), 1957–1992, doi:10.5194/bgd-10-1957-
985 2013.

986 Mitchell, P. J., P. N. J. Lane, and R. G. Benyon (2011), Capturing within catchment variation in
987 evapotranspiration from montane forests using LiDAR canopy profiles with measured and
988 modelled fluxes of water, *Ecohydrol.*, 5(6), 708–720, doi:10.1002/eco.255.

989 Moeser, D., J. Roubinek, P. Schleppei, F. Morsdorf, and T. Jonas (2014), Canopy closure, LAI
990 and radiation transfer from airborne LiDAR synthetic images, *Agricultural and Forest*
991 *Meteorology*, 197(0), 158–168, doi:10.1016/j.agrformet.2014.06.008.

992 Mora, B., M. A. Wulder, G. W. Hobart, J. C. White, C. W. Bater, F. A. Gougeon, A. Varhola,
993 and N. C. Coops (2013), Forest inventory stand height estimates from very high spatial
994 resolution satellite imagery calibrated with LiDAR plots, *International Journal of Remote*
995 *Sensing*, 34(12), 4406–4424, doi:10.1080/01431161.2013.779041.

996 Mundt, J. T., D. R. Streutker, and N. F. Glenn (2006), Mapping Sagebrush Distribution Using
997 Fusion of Hyperspectral and LiDAR Classifications, *Photogrammetric engineering and*
998 *remote sensing*, 72(1), 47–54, doi:10.14358/PERS.72.1.47.

999 Musselman, K. N., S. A. Margulis, and N. P. Molotch (2013), Estimation of solar direct beam
1000 transmittance of conifer canopies from airborne LiDAR, *Remote Sensing of Environment*,
1001 136(0), 402–415, doi:10.1016/j.rse.2013.05.021.

1002 Næsset, E. and T. Gobakken (2005). Estimating forest growth using canopy metrics derived from
1003 airborne laser scanner data, *Remote sensing of environment*, 96(3), 453-465, doi:
1004 10.1016/j.rse.2005.04.001.

1005 Nathanson, M., J. W. Kean, T. J. Grabs, J. Seibert, H. Laudon, and S. W. Lyon (2012),
1006 Modelling rating curves using remotely sensed LiDAR data, *Hydrol. Process.*, 26(9), 1427–
1007 1434, doi:10.1002/hyp.9225.

1008 National Research Council (2012), *New Research Opportunities in the Earth Sciences*, National
1009 Academy Press, Washington D.C.

1010 Nissen, E., T. Maruyama, J.R. Arrowsmith, J.R. Elliott, A.K. Krishnan, M.E. Oskin, and S.
1011 Saripalli (2014), Coseismic fault zone deformation revealed with differential lidar: examples

1012 from Japanese Mw ~7 intraplate earthquakes, *Earth and Planetary Science Letters*, 405,
1013 244-256, doi: doi:10.1016/j.epsl.2014.08.031.

1014 Nissen, E., A. K. Krishnan, J. R. Arrowsmith, and S. Saripalli (2012), Three-dimensional surface
1015 displacements and rotations from differencing pre- and post-earthquake LiDAR point clouds,
1016 *Geophysical Research Letters*, 39(16), L16301, doi:10.1029/2012GL052460.

1017 Olsoy, P. J., N. F. Glenn, P. E. Clark, and D. R. Derryberry (2014), Aboveground total and green
1018 biomass of dryland shrub derived from terrestrial laser scanning, *ISPRS Journal of*
1019 *Photogrammetry and Remote Sensing*, 88(0), 166–173, doi:10.1016/j.isprsjprs.2013.12.006.

1020 Oskin, M. E. et al. (2012), Near-Field Deformation from the El Mayor–Cucapah Earthquake
1021 Revealed by Differential LIDAR, *Science*, 335(6069), 702–705,
1022 doi:10.1126/science.1213778.

1023 Palminteri, S., G. V. N. Powell, G. P. Asner, and C. A. Peres (2012), LiDAR measurements of
1024 canopy structure predict spatial distribution of a tropical mature forest primate, *Remote*
1025 *Sensing of Environment*, 127(0), 98–105, doi:10.1016/j.rse.2012.08.014.

1026 Passalacqua, P., P. Tarolli, and E. Foufoula-Georgiou (2010), Testing space-scale methodologies
1027 for automatic geomorphic feature extraction from LiDAR in a complex mountainous
1028 landscape, *Water Resources Research*, 46(11), W11535, doi:10.1029/2009WR008812.

1029 Pelletier, J. D. (2013), Deviations from self-similarity in barchan form and flux: The case of the
1030 Salton Sea dunes, California, *J. Geophys. Res. Earth Surf.*, 118(4), 2013JF002867,
1031 doi:10.1002/2013JF002867.

1032 Pelletier, J. D. et al. (2013), Coevolution of nonlinear trends in vegetation, soils, and topography
1033 with elevation and slope aspect: A case study in the sky islands of southern Arizona, *J.*
1034 *Geophys. Res. Earth Surf.*, 118(2), 741–758, doi:10.1002/jgrf.20046.

1035 Pelletier, J. D., and C. A. Orem (2014), How do sediment yields from post-wildfire debris-laden
1036 flows depend on terrain slope, soil burn severity class, and drainage basin area? Insights
1037 from airborne-LiDAR change detection, *Earth Surface Processes and Landforms*, n/a–n/a,
1038 doi:10.1002/esp.3570.

1039 Pelletier, J. D., and J. T. Perron (2012), Analytic solution for the morphology of a soil-mantled
1040 valley undergoing steady headward growth: Validation using case studies in southeastern
1041 Arizona, *Journal of Geophysical Research: Earth Surface (2003--2012)*, 117(F2),
1042 doi:10.1029/2011JF002281.

1043 Pelletier, J. D., S. B. DeLong, C. A. Orem, P. Becerra, K. Compton, K. Gressett, J. Lyons-Baral,
1044 L. A. McGuire, J. L. Molaro, and J. C. Spinler (2012), How do vegetation bands form in dry
1045 lands? Insights from numerical modeling and field studies in southern Nevada, USA,
1046 *Journal of Geophysical Research: Atmospheres (1984–2012)*, 117(F4), F04026,
1047 doi:10.1029/2012JF002465.

1048 Perignon, M. C., G. E. Tucker, E. R. Griffin, and J. M. Friedman (2013), Effects of riparian
1049 vegetation on topographic change during a large flood event, Rio Puerco, New Mexico,
1050 USA, *J. Geophys. Res. Earth Surf.*, 118(3), 1193–1209, doi:10.1002/jgrf.20073.

1051 Perron, J. T., and J. L. Hamon (2012), Equilibrium form of horizontally retreating, soil-mantled
1052 hillslopes: Model development and application to a groundwater sapping landscape, *Journal*
1053 *of Geophysical Research: Atmospheres (1984–2012)*, 117(F1), F01027,
1054 doi:10.1029/2011JF002139.

1055 Perron, J. T., J. W. Kirchner, and W. E. Dietrich (2008), Spectral signatures of characteristic
1056 spatial scales and nonfractal structure in landscapes, *Journal of Geophysical Research:*
1057 *Atmospheres (1984–2012)*, 113(F4), F04003, doi:10.1029/2007JF000866.

1058 Persson, A., A. Hasan, J. Tang, and P. Pilesjö (2012), Modelling Flow Routing in Permafrost
1059 Landscapes with TWI: An Evaluation against Site-Specific Wetness Measurements,
1060 *Transactions in GIS*, 16(5), 701–713, doi:10.1111/j.1467-9671.2012.01338.x.

1061 Plotnick, R. E., R. H. Gardner, W. W. Hargrove, K. Prestegard, and M. Perlmutter (1996),
1062 Lacunarity analysis: A general technique for the analysis of spatial patterns, *Phys. Rev. E*,
1063 53(5), 5461–5468, doi:10.1103/PhysRevE.53.5461.

1064 Rengers, F. K., and G. E. Tucker (2014), Analysis and modeling of gully headcut dynamics,
1065 North American high plains, *J. Geophys. Res. Earth Surf.*, 119(5), 983–1003,
1066 doi:10.1002/2013JF002962.

1067 Rhoades, E. L., M. A. O'Neal, and J. E. Pizzuto (2009), Quantifying bank erosion on the South
1068 River from 1937 to 2005, and its importance in assessing Hg contamination, *Applied*
1069 *Geography*, 29(1), 125–134, doi:10.1016/j.apgeog.2008.08.005.

1070 Riaño, D., F. Valladares, S. Condés, and E. Chuvieco (2004), Estimation of leaf area index and
1071 covered ground from airborne laser scanner (LiDAR) in two contrasting forests, *Agricultural*
1072 *and Forest Meteorology*, 124(3–4), 269–275, doi:10.1016/j.agrformet.2004.02.005.

1073 Richardson, J. J., L. M. Moskal, and S.-H. Kim (2009), Modeling approaches to estimate

1074 effective leaf area index from aerial discrete-return LIDAR, *Agricultural and Forest*
1075 *Meteorology*, 149(6–7), 1152–1160, doi:10.1016/j.agrformet.2009.02.007.

1076 Roering, J. J. (2008), How well can hillslope evolution models “explain” topography?
1077 Simulating soil transport and production with high-resolution topographic data, *Geological*
1078 *Society of America Bulletin*, 120(9-10), 1248–1262, doi:10.1130/B26283.1.

1079 Roering, J. J., B. H. Mackey, J. A. Marshall, K. E. Sweeney, N. I. Deligne, A. M. Booth, A. L.
1080 Handwerger, and C. Cerovski-Darriau (2013), “You are HERE”: Connecting the dots with
1081 airborne LiDAR for geomorphic fieldwork, *Geomorphology*, 200(0), 172–183,
1082 doi:10.1016/j.geomorph.2013.04.009.

1083 Roering, J. J., J. Marshall, A. M. Booth, M. Mort, and Q. Jin (2010), Evidence for biotic controls
1084 on topography and soil production, *Earth and Planetary Science Letters*, 298(1–2), 183–190,
1085 doi:10.1016/j.epsl.2010.07.040.

1086 Roering, J. J., L. L. Stimely, B. H. Mackey, and D. A. Schmidt (2009), Using DInSAR, airborne
1087 LiDAR, and archival air photos to quantify landsliding and sediment transport, *Geophysical*
1088 *Research Letters*, 36(19), L19402, doi:10.1029/2009GL040374.

1089 Sankey, J. B., D. J. Law, D. D. Breshears, S. M. Munson, and R. H. Webb (2013), Employing
1090 LiDAR to detail vegetation canopy architecture for prediction of aeolian transport,
1091 *Geophysical Research Letters*, 40(9), 1724–1728, doi:10.1002/grl.50356.

1092 Sankey, J. B., N. F. Glenn, M. J. Germino, A. I. N. Gironella, and G. D. Thackray (2010),
1093 Relationships of aeolian erosion and deposition with LiDAR-derived landscape surface
1094 roughness following wildfire, *Geomorphology*, 119(1–2), 135–145,
1095 doi:10.1016/j.geomorph.2010.03.013.

1096 Schimel, D. S., G.P. Asner, and P. Moorcroft (2013), Observing changing ecological diversity in
1097 the Anthropocene, *Frontiers in Ecology and the Environment*, 11(3), 129-137, doi:
1098 10.1890/120111

1099 Seidel, D., S. Fleck, C. Leuschner, and T. Hammett (2011), Review of ground-based methods to
1100 measure the distribution of biomass in forest canopies, *Annals of Forest Science*, 68(2), 225–
1101 244, doi:10.1007/s13595-011-0040-z.

1102 Shook, K., J. W. Pomeroy, C. Spence, and L. Boychuk (2013), Storage dynamics simulations in
1103 prairie wetland hydrology models: evaluation and parameterization, *Hydrol. Process.*,
1104 27(13), 1875–1889, doi:10.1002/hyp.9867.

1105 Simard, M., N. Pinto, J. B. Fisher, and A. Baccini (2011), Mapping forest canopy height globally
1106 with spaceborne LiDAR, *Journal of Geophysical Research: Atmospheres (1984–2012)*,
1107 116(G4), G04021, doi:10.1029/2011JG001708.

1108 Snyder, N. P. (2009), Studying Stream Morphology With Airborne Laser Elevation Data, *Eos*,
1109 *Transactions American Geophysical Union*, 90(6), 45–46, doi:10.1029/2009EO060001.

1110 Staley, D. M., T. A. Wasklewicz, and J. W. Kean (2014), Characterizing the primary material
1111 sources and dominant erosional processes for post-fire debris-flow initiation in a headwater
1112 basin using multi-temporal terrestrial laser scanning data, *Geomorphology*, 214(0), 324–338,
1113 doi:10.1016/j.geomorph.2014.02.015.

1114 Stennett, T. A. (2004), LiDAR: Strap in tight, and prepare to go vertical, *Photogrammetric*
1115 *engineering and remote sensing*, 70(5), 545–548.

1116 Stout, J. C., and P. Belmont (2014), TerEx Toolbox for semi-automated selection of fluvial
1117 terrace and floodplain features from LiDAR, *Earth Surface Processes and Landforms*, 39(5),
1118 569–580, doi:10.1002/esp.3464.

1119 Streutker, D. R., and N. F. Glenn (2006), LiDAR measurement of sagebrush steppe vegetation
1120 heights, *Remote Sensing of Environment*, 102(1–2), 135–145, doi:10.1016/j.rse.2006.02.011.

1121 Sørensen, R., and J. Seibert (2007), Effects of DEM resolution on the calculation of
1122 topographical indices: TWI and its components, *Journal of Hydrology*, 347(1–2), 79–89,
1123 doi:10.1016/j.jhydrol.2007.09.001.

1124 Tarolli, P. (2014), High-resolution topography for understanding Earth surface processes:
1125 Opportunities and challenges, *Geomorphology*, 216(0), 295–312,
1126 doi:10.1016/j.geomorph.2014.03.008.

1127 Tenenbaum, D. E., L. E. Band, S. T. Kenworthy, and C. L. Tague (2006), Analysis of soil
1128 moisture patterns in forested and suburban catchments in Baltimore, Maryland, using high-
1129 resolution photogrammetric and LIDAR digital elevation datasets, *Hydrol. Process.*, 20(2),
1130 219–240, doi:10.1002/hyp.5895.

1131 Thoma, D. P., S. C. Gupta, M. E. Bauer, and C. E. Kirchoff (2005), Airborne laser scanning for
1132 riverbank erosion assessment, *Remote Sensing of Environment*, 95(4), 493–501,
1133 doi:10.1016/j.rse.2005.01.012.

1134 Tinkham, W. T., A. M. S. Smith, H.-P. Marshall, T. E. Link, M. J. Falkowski, and A. H.
1135 Winstral (2014), Quantifying spatial distribution of snow depth errors from LiDAR using

1136 Random Forest, *Remote Sensing of Environment*, 141(0), 105–115,
 1137 doi:10.1016/j.rse.2013.10.021.

1138 Trujillo, E., J. A. Ramírez, and K. J. Elder (2009), Scaling properties and spatial organization of
 1139 snow depth fields in sub-alpine forest and alpine tundra, *Hydrol. Process.*, 23(11), 1575–
 1140 1590, doi:10.1002/hyp.7270.

1141 Varhola, A., and N. C. Coops (2013), Estimation of watershed-level distributed forest structure
 1142 metrics relevant to hydrologic modeling using LiDAR and Landsat, *Journal of Hydrology*,
 1143 487(0), 70–86, doi:10.1016/j.jhydrol.2013.02.032.

1144 Varhola, A., N. C. Coops, Y. Alila, and M. Weiler (2014), Exploration of remotely sensed forest
 1145 structure and ultrasonic range sensor metrics to improve empirical snow models, *Hydrol.*
 1146 *Process.*, 28(15), 4433–4448, doi:10.1002/hyp.9952.

1147 Vierling, K. T., L. A. Vierling, W. A. Gould, S. Martinuzzi, and R. M. Clawges (2008), LiDAR:
 1148 shedding new light on habitat characterization and modeling, *Frontiers in Ecology and the*
 1149 *Environment*, 6(2), 90–98, doi:10.1890/070001.

1150 Vosselman, G., and H.-G. Maas (2010), *Airborne and terrestrial laser scanning*, CRC Press,
 1151 London.

1152 Wagner, W., M. Hollaus, C. Briese, and V. Ducic (2008), 3D vegetation mapping using small-
 1153 footprint full-waveform airborne laser scanners, *International Journal of Remote Sensing*,
 1154 29(5), 1433–1452, doi:10.1080/01431160701736398.

1155 Wallace, L., A. Lucieer, C. Watson, and D. Turner (2012), Development of a UAV-LiDAR
 1156 System with Application to Forest Inventory, *Remote Sensing*, 4(6), 1519–1543,
 1157 doi:10.3390/rs4061519.

1158 Wedding, L. M., A. M. Friedlander, M. McGranaghan, R. S. Yost, and M. E. Monaco (2008),
 1159 Using bathymetric LiDAR to define nearshore benthic habitat complexity: Implications for
 1160 management of reef fish assemblages in Hawaii, *Remote Sensing of Environment*, 112(11),
 1161 4159–4165, doi:10.1016/j.rse.2008.01.025.

1162 West, N., E. Kirby, P. Bierman, and B. A. Clarke (2014), Aspect-dependent variations in regolith
 1163 creep revealed by meteoric ¹⁰Be, *Geology*, 42(6), 507–510, doi:10.1130/G35357.1.

1164 Westoby, M. J., J. Brasington, N. F. Glasser, M. J. Hambrey, and J. M. Reynolds (2012),
 1165 “Structure-from-Motion” photogrammetry: A low-cost, effective tool for geoscience
 1166 applications, *Geomorphology*, 179(0), 300–314, doi:10.1016/j.geomorph.2012.08.021.

1167 Wheaton, J. M., J. Brasington, S. E. Darby, and D. A. Sear (2010), Accounting for uncertainty in
1168 DEMs from repeat topographic surveys: improved sediment budgets, *Earth Surface*
1169 *Processes and Landforms*, 35(2), 136–156, doi:10.1002/esp.1886.

1170 Williams, G. D. et al. (2013), Beyond Point Measurements: Sea Ice Floes Characterized in 3-D,
1171 *Eos, Transactions American Geophysical Union*, 94(7), 69–70, doi:10.1002/2013EO070002.

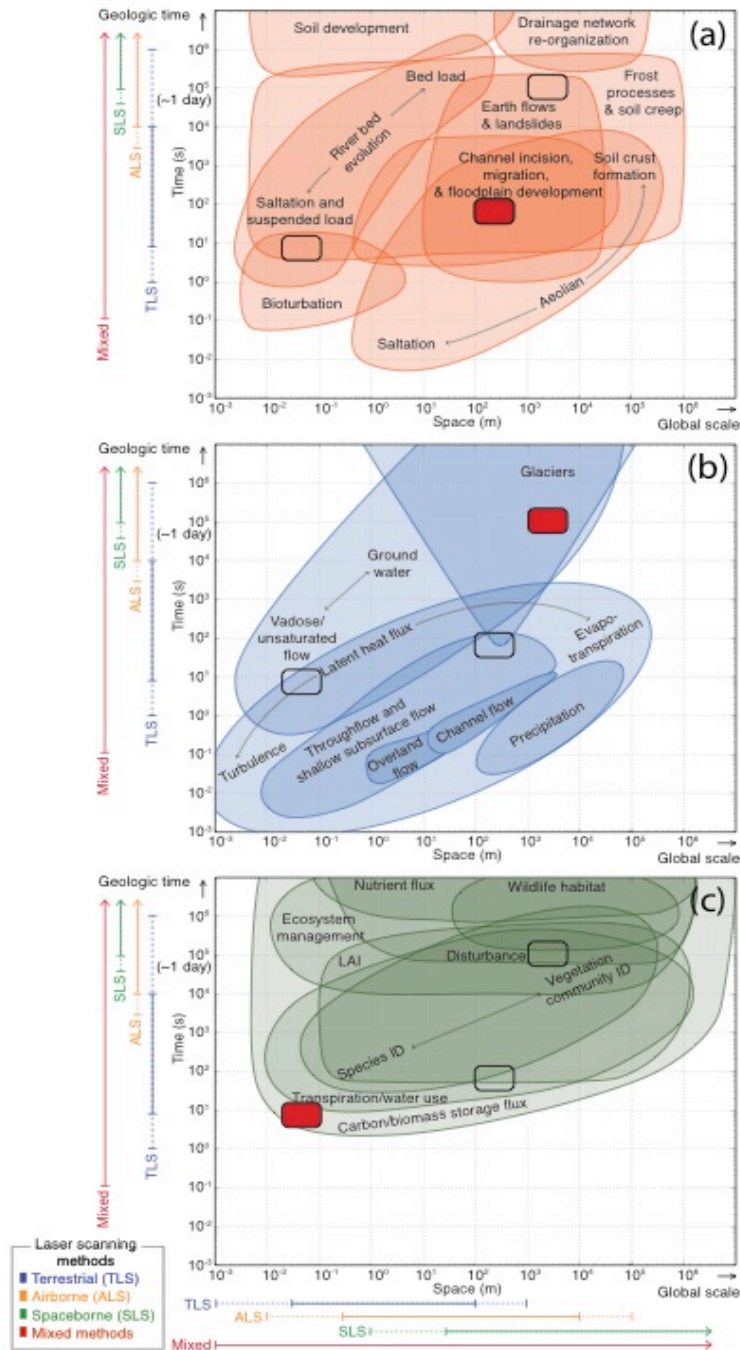
1172 Wulder, M. A., J. C. White, R. F. Nelson, E. Næsset, H. O. Ørka, N. C. Coops, T. Hilker, C. W.
1173 Bater, and T. Gobakken (2012), LiDAR sampling for large-area forest characterization: A
1174 review, *Remote Sensing of Environment*, 121(0), 196–209, doi:10.1016/j.rse.2012.02.001.

1175 Young, A. P., M. J. Olsen, N. Driscoll, R. E. Flick, R. Gutierrez, R. T. Guza, E. Johnstone, and
1176 F. Kuester (2010), Comparison of Airborne and Terrestrial LiDAR Estimates of Seacliff
1177 Erosion in Southern California, *Photogrammetric engineering and remote sensing*, 76(4),
1178 421–427, doi:10.14358/PERS.76.4.421.

1179 Yu, X., J. Hyyppä, H. Kaartinen, and M. Maltamo (2004), Automatic detection of harvested trees
1180 and determination of forest growth using airborne laser scanning, *Remote Sensing of*
1181 *Environment*, 90(4), 451–462, doi:10.1016/j.rse.2004.02.001.

1182 Zellweger, F., F. Morsdorf, R. Purves, V. Braunisch, and K. Bollmann (2014), Improved
1183 methods for measuring forest landscape structure: LiDAR complements field-based habitat
1184 assessment, *Biodivers Conserv*, 23(2), 289–307, doi:10.1007/s10531-013-0600-7.

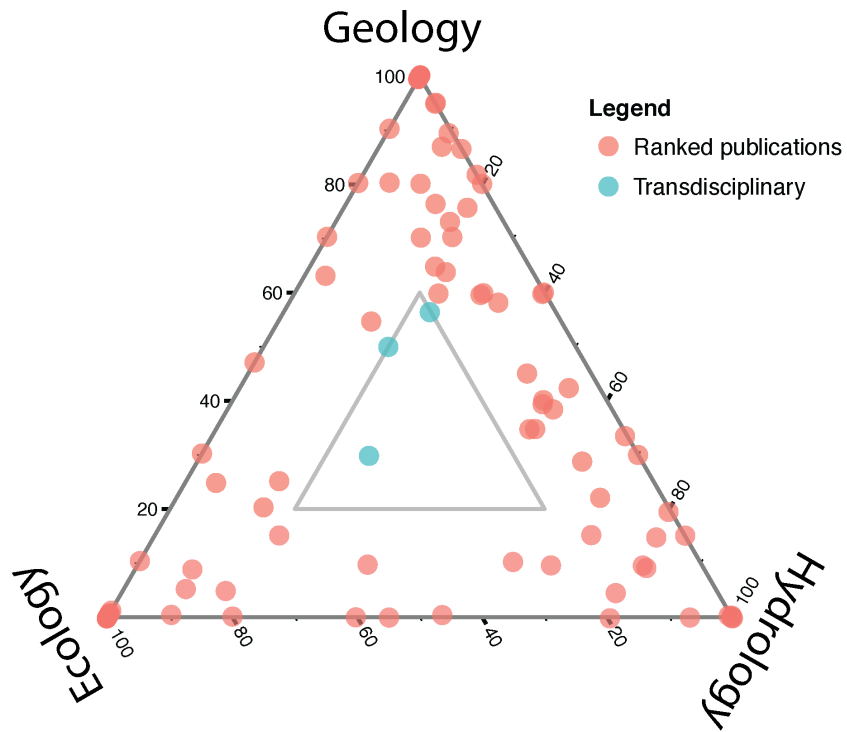
1185 Zhao, K., S. Popescu, and R. Nelson (2009), LiDAR remote sensing of forest biomass: A scale-
1186 invariant estimation approach using airborne lasers, *Remote Sensing of Environment*, 113(1),
1187 182–196, doi:10.1016/j.rse.2008.09.009.



1188

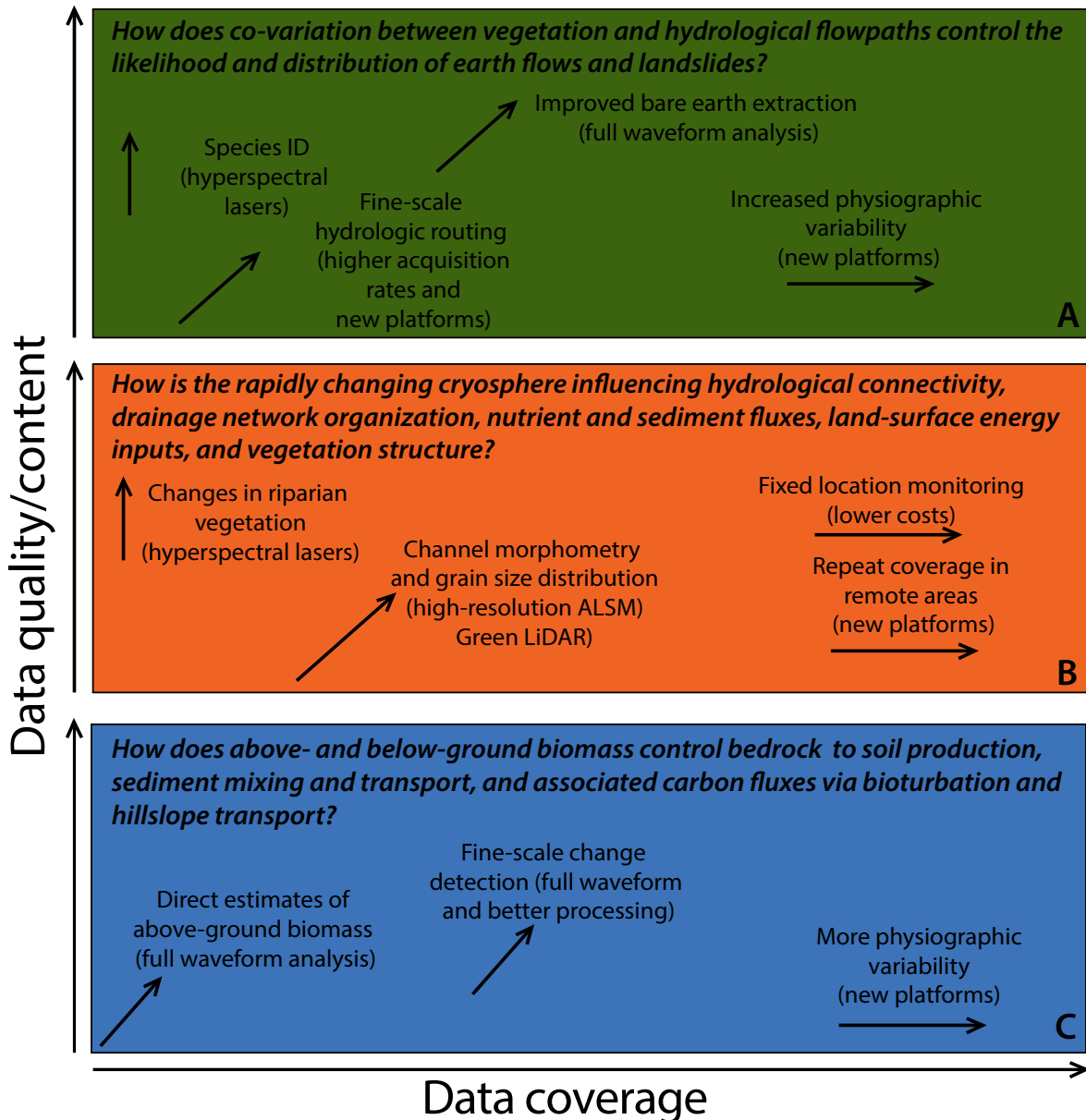
1189 **Figure 1.** Important CZ processes graphed as a function of time versus space for geomorphology
 1190 (a), hydrology (b), and ecology (c). The spatial and temporal scales that lidar is currently
 1191 addressing are shown as colored bars, with dotted bars indicating increasing resolutions and
 1192 larger extents available in the next five years. Overlapping spatiotemporal scales that encompass
 1193 the example questions in the Figure 3 are also noted with red boxes.

1194



1195
 1196
 1197
 1198
 1199
 1200
 1201
 1202

Figure 2. Depiction of the disciplinary focus of 147 journal articles using lidar. Articles were qualitatively ranked based on their applicability to geomorphological, hydrological, and/or ecological process understanding. Articles in the center are examples of transdisciplinary lidar applications, with those shown in blue used as exemplars in the text.



1203
 1204
 1205
 1206
 1207
 1208
 1209
 1210
 1211

Figure 3. Example CZ research questions conceptualizing the transdisciplinary potential of lidar datasets when coupled with future technological advances. The questions encompass processes from geomorphology (a), hydrology (b), and ecology (c) that overlap spatial and temporal scales. These scales are noted in Figure 1. The text in the panel notes specific improvements offered and the technology needed in parentheses. The arrows qualitatively represent whether the technological advance expands data coverage and/or data quality/content.